Oregon State University

COLLEGE OF ENGINEERING | School of Mechanical, Industrial, and Manufacturing Engineering

Laser directed energy deposition of Ni-based superalloy GRCop42 joints for multi-metal components

PhD Final Examination

Mechanical Engineering with Advanced Manufacturing Option

PhD Student: Jakub (Kuba) Preis

Advisor: Dr. Somayeh Pasebani

Committee: Dr. Brian Paul, Dr. Donghua Xu, Dr. Julie Tucker, Dr. David H McIntyre

About the presenter

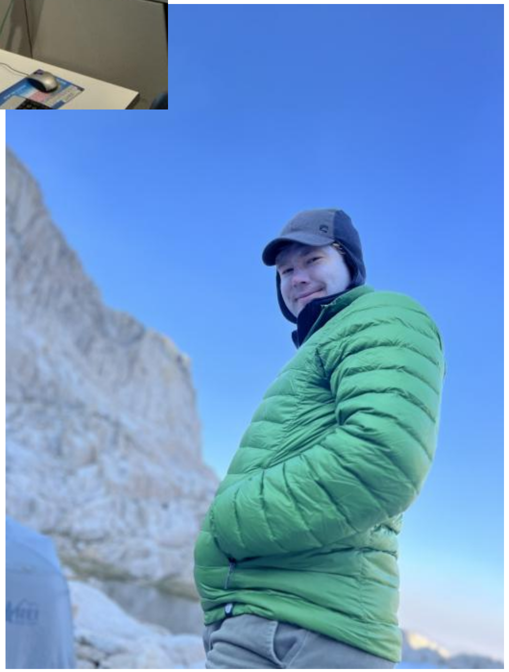

2015 - 2019 B.S. Manufacturing Engineering
California Polytechnic State University, San Luis Obispo, CA, USA

2019 - 2020 Additive Manufacturing Engineer
Divergent Technologies, Los Angeles, CA, USA

2020 - 2021 Additive Manufacturing Engineer
Divergent Technologies, on assignment to SLM solutions, Lubeck, Germany

2021 - Present Graduate Research Assistant
Oregon State University, Corvallis, OR, USA

Hobbies: Biking, hiking, anything that has to do with the outdoors.

Pre-Industrial printing/manufacturing

2 dimensional

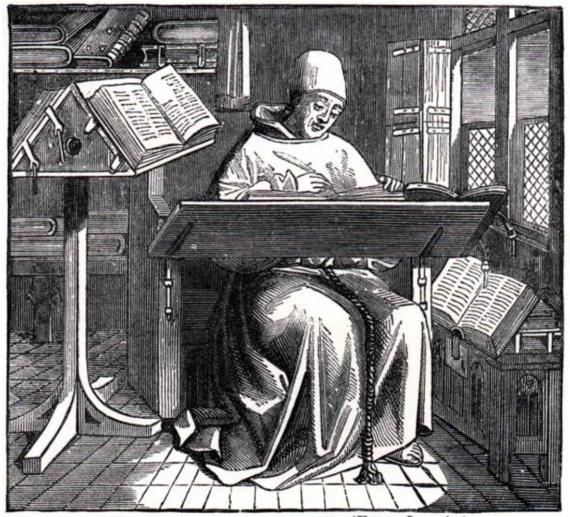
SCRIPTORIUM MONK AT WORK. (From *Lacroix.*)

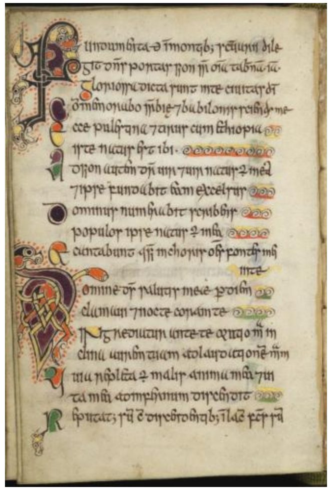
Scottland's Book of Kells, 800 AD

Disadvantages :

- Not repeatable (every book is different).
- Expensive and slow.
    - Every book must copied/written made by a trained expert.

3 dimensional

Disadvantages :

- Not repeatable (every part is different).
- Expensive and slow.
    - Every part must be made by an trained expert.

Industrial printing/manufacturing

2 dimensional

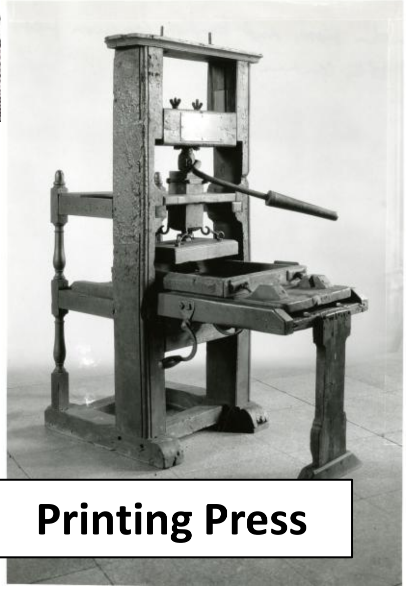

Printing Press

Gutenberg bible
1455 AD

Advantages:

- Repeatable.
- Faster than manual copying.

Disadvantages:

- Each setup is page-specific.
- Cannot print all images.

3 dimensional

Traditional Manufacturing

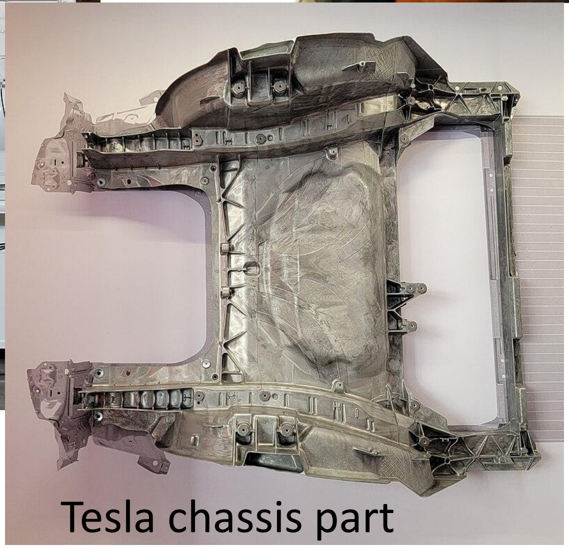

Tesla chassis part

Advantages:

- Repeatable.
- Better quality.
- Faster than manual manufacturing.

Disadvantages :

- Requires geometry specific tooling (large fixed cost).
- Cannot fabricate all geometries (assemblies required).

Modern printing/manufacturing

2 dimensional


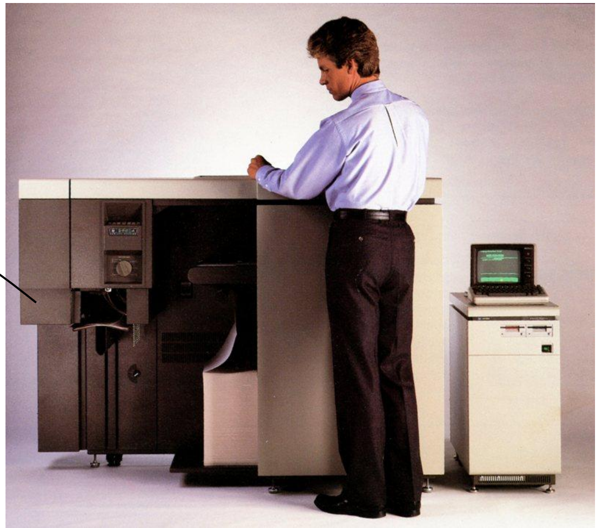

Inkjet printer (black and white)

Advantages:
- Do not need to change configuration each page.

Disadvantages :
- Slow.
- Only black and white.

3 dimensional

Additive Manufacturing (AM)

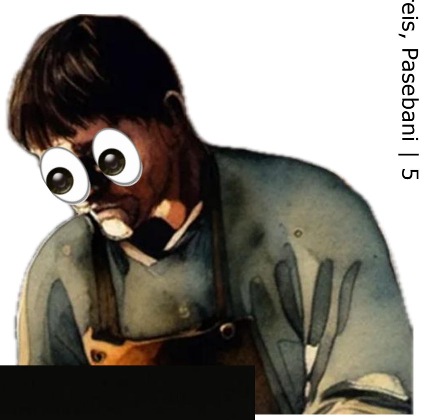


GE fuel nozzle

Advantages:
- Greater design freedom (can print more geometries).
- No tooling, machine is not geometry specific.

Disadvantages :
- Slow.
- Constrained to one material.

Advantages of AM over traditional manufacturing

Increased use of additive manufacturing

Next generation printing/manufacturing

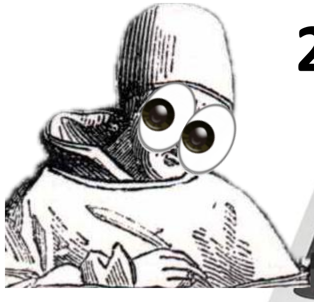

2 dimensional

Laser printer (color)

3 dimensional

Next generation AM machines

Rocket Exhaust Chamber + Nozzle (NASA)

Advantages:
- Can essentially print any design.
- **Can print color.**

Advantages:
- Higher deposition rate (faster printing).
- Multi-material capability.

Constraints:
- Part resolution.
- **Metallurgical constraints.**

Thermal management of Ni-based superalloys

- The joining of Inconel superalloys to high temp Cu alloys is of interest in applications which require both regions **of high temperature strength** and **high thermal conductivity**.

Rocket Exhaust Chamber [1]
NASA Marshall Space Flight Center

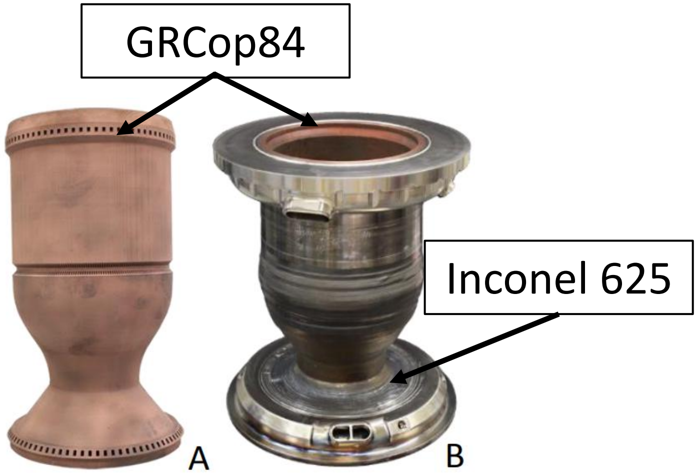

Rocket Exhaust Chamber + Nozzle [2]
NASA Marshall Space Flight Center

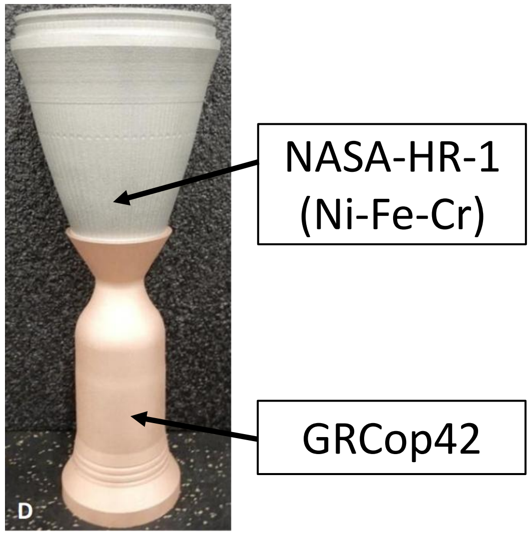

Superheater Concept
Oregon State University

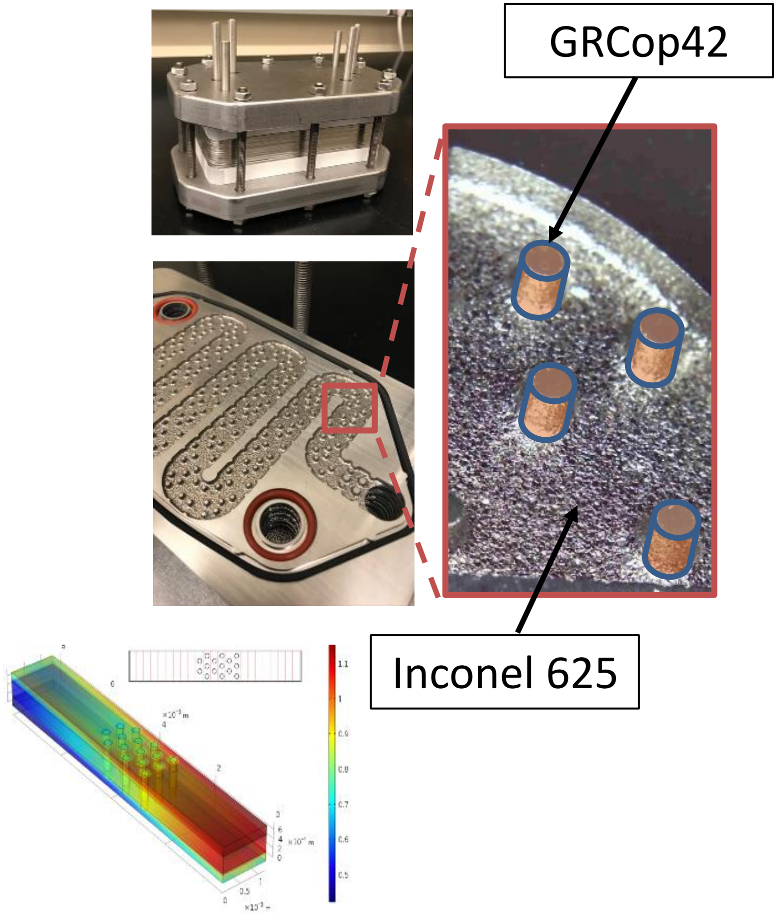

Alloy	Thermal Conductivity [W/mK]	UTS, 25 C [MPa]	UTS, 650 C [MPa]
Inconel 625	10 [5]	1121 [4]	637 [6]
GRCop42	275 [3]	360 [3]	85 [1]

[1] Paul R. Gradl, Christopher S. Protz, David L. Ellis, and Sandy E. Greene. "Progress in additively manufactured copper-alloy GRCOP-84, GRCOP-42, and bimetallic combustion chambers for liquid rocket engines". In: Proceedings of the International Astronautical Congress, IAC. Vol. 2019-October. 2019.
[2] Paul R. Gradl, Chris Protz, John Fikes, Allison Clark, Laura Evans, Sandi Miller, David Ellis, and Tyler Hudson. "Lightweight thrust chamber assemblies using multi-alloy additive manufacturing and composite over-wrap". In:AIAA Propulsion and Energy 2020 Forum. 2020.
[3] Paul R. Gradl, Christopher S. Protz, David L. Ellis, and Sandy E. Greene. "Progress in additively manufactured copper-alloy GRCOP-84, GRCOP-42, and bimetallic combustion chambers for liquid rocket engines". In: Proceedings of the International Astronautical Congress, IAC. Vol. 2019-October. 2019.
[4] MD Ashabul Anam. "Microstructure and mechanical properties of selective laser melted superalloy Inconel 625." In: Elsevier (2018).
[5] Asit Kumar Parida and Kalipada Maity. "Comparison the machinability of Inconel 718, Inconel 625 and Monel 400 in hot turning operation". In: Engineering Science and Technology, an International Journal 21.3 (June2018), pp. 364–370. issn: 2215-0986. doi:10.1016/J.JESTCH.2018.03.018.11
[6] : Kim K-Sik, Kang T-Hoon, Kassner ME, Son K-Tae, Lee K-Ahn, High-Temperature Tensile and High Cycle Fatigue Properties of Inconel 625 Alloy Manufactured by Laser Powder Bed Fusion, Additive Manufacturing (2020), doi: https://doi.org/10.1016/j.addma.2020.101377

Outline

Goal: Understand the process-structure-property relationship in Inconel – GRCop42 joints

- Impact of parameters for LDED processing of wire Inconel 625
  - ❖ Manuscript 1: *Preis et al., Influence of travel speed on microstructure and mechanical behavior of Inconel 625 fabricated using wire fed laser directed energy deposition, Journal of Materials Processing Technology*

- Impact of Inconel 625 GRCop42 mixing
  - ❖ Manuscript 2: *Preis et al., Effect of Liquid Miscibility Gap on Defects in Inconel 625–GRCop42 Joints through Analysis of Gradient Composition Microstructure, Journal of Manufacturing and Materials Processing*

Inconel 625 GRCop42 mixtures

- Bimetallic joining of Inconel 625 with GRCop42 using LDED
  - ❖ Manuscript 3: *Preis et al., Effect of laser power and deposition sequence on microstructure of GRCop42 - Inconel 625 joints fabricated using laser directed energy deposition, Materials and Design*

- Development of a filler composition for joining of Inconel 718 with GRCop42 and LDED printing
  - ❖ Manuscript 4: *Microstructure, microhardness, and thermal properties of Inconel 718 - GRCop42 joint with liquid miscibility gap avoiding filler compositions*

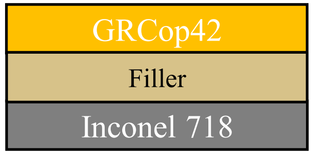

Outline

Goal: Understand the process-structure-property relationship in Inconel – GRCop42 joints

- Impact of parameters for LDED processing of wire Inconel 625
  - ❖ Manuscript 1: *Preis et al., Influence of travel speed on microstructure and mechanical behavior of Inconel 625 fabricated using wire fed laser directed energy deposition, Journal of Materials Processing Technology*

- Impact of Inconel 625 GRCop42 mixing
  - ❖ Manuscript 2: *Preis et al., Effect of Liquid Miscibility Gap on Defects in Inconel 625–GRCop42 Joints through Analysis of Gradient Composition Microstructure, Journal of Manufacturing and Materials Processing*

Inconel 625 GRCop42 mixtures

- Bimetallic joining of Inconel 625 with GRCop42 using LDED
  - ❖ Manuscript 3: *Preis et al., Effect of laser power and deposition sequence on microstructure of GRCop42 - Inconel 625 joints fabricated using laser directed energy deposition, Materials and Design*

- Development of a filler composition for joining of Inconel 718 with GRCop42 and LDED printing
  - ❖ Manuscript 4: *Microstructure, microhardness, and thermal properties of Inconel 718 - GRCop42 joint with liquid miscibility gap avoiding filler compositions*

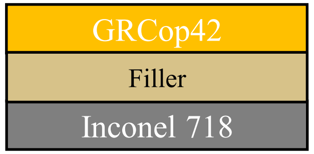

Key terms

- Directed Energy Deposition

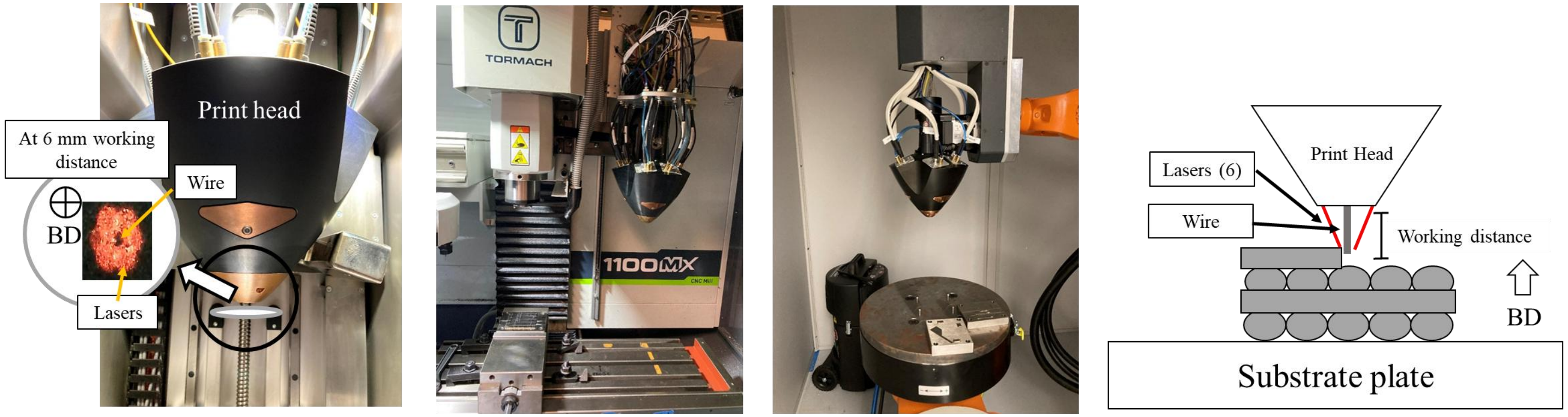

(a) (b) (c) (d)

- Travel speed – the linear speed (typically in mm/min) at which a laser exposes a given pass.
- Laser power – the power (typically in Watts) used during the exposure of a given pass.

Wire LDED of Inconel 625

- Meltio M450 wire-power system used
  - Advantages of wire LDED:100% of material utilized, relatively fast print speed
- Processing map developed for single track deposition.
- A high-travel-speed and low-travel speed parameter selected for microstructure and mechanical property characterization.

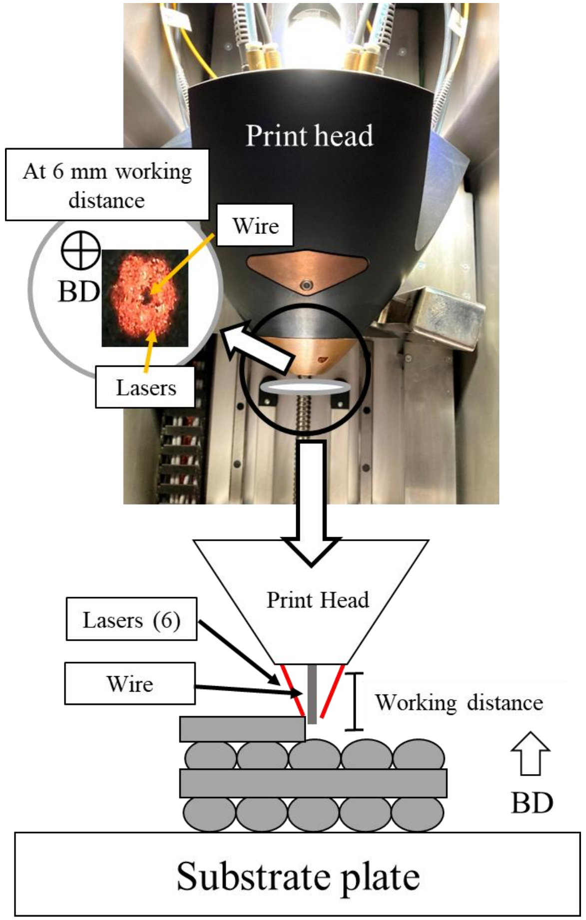

Alloy	Ni	Cr	Nb	Ta	Mo	Cu	Fe	Ti	Al	Other
Inconel 625	**64.8**	**22.2**	**3.49**		**8.6**	.016	0.26	0.21	0.14	.284

Preis et al., Influence of travel speed on microstructure and mechanical behavior of Inconel 625 fabricated using wire fed laser directed energy deposition (2024)

Single and Multi Track Experiments

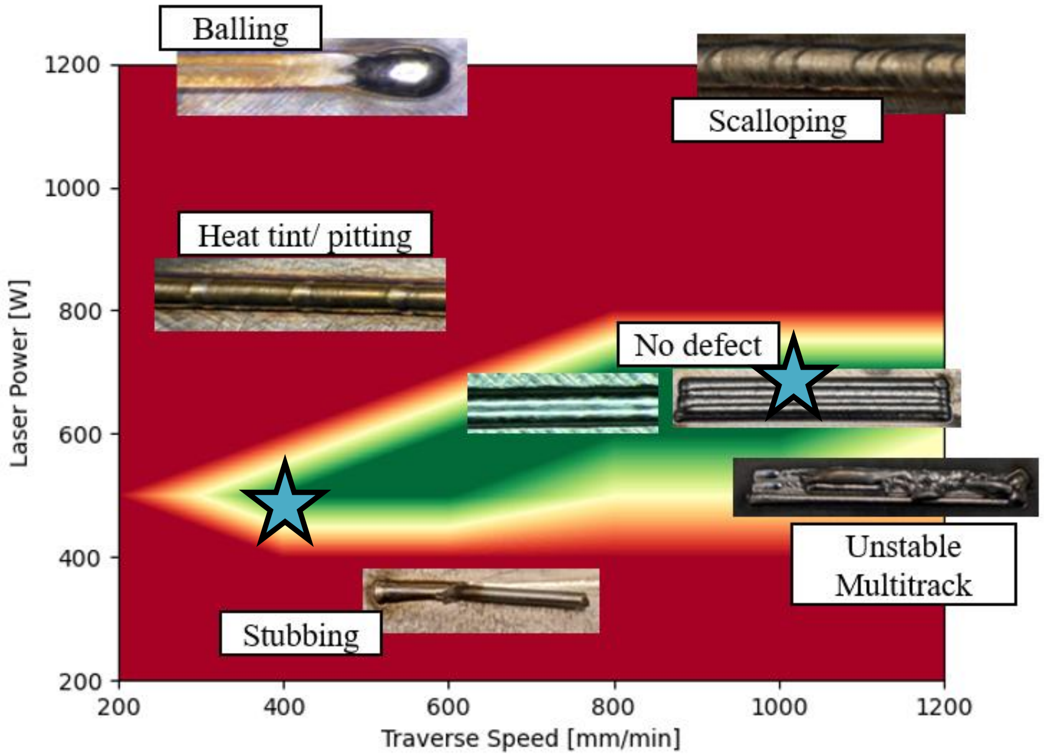

- Parameter space of defect free single and multi tracks shown in green.
- Multi track defect mode consisted of **inability to change direction** and occurred at **high speed**.
- A overlap ration (ratio of hatch spacing to bead width) of 0.7 found to be optimal for multi tracks.
- **High-travel-speed** and **low-travel speed** parameters identified for further characterization.

Parameter	**Laser Power** *W*	**Travel Speed** *mm/min*
Low-travel-speed	500	400
High-travel-speed	700	1000

Preis et al., Influence of travel speed on microstructure and mechanical behavior of Inconel 625 fabricated using wire fed laser directed energy deposition (2024)

Microstructural characterization

- **Columnar grains** observed in the low-travel-speed sample.
- **Columnar + equiaxed grains** observed in the high-travel-speed sample.
- Epitaxial growth observed in both samples.

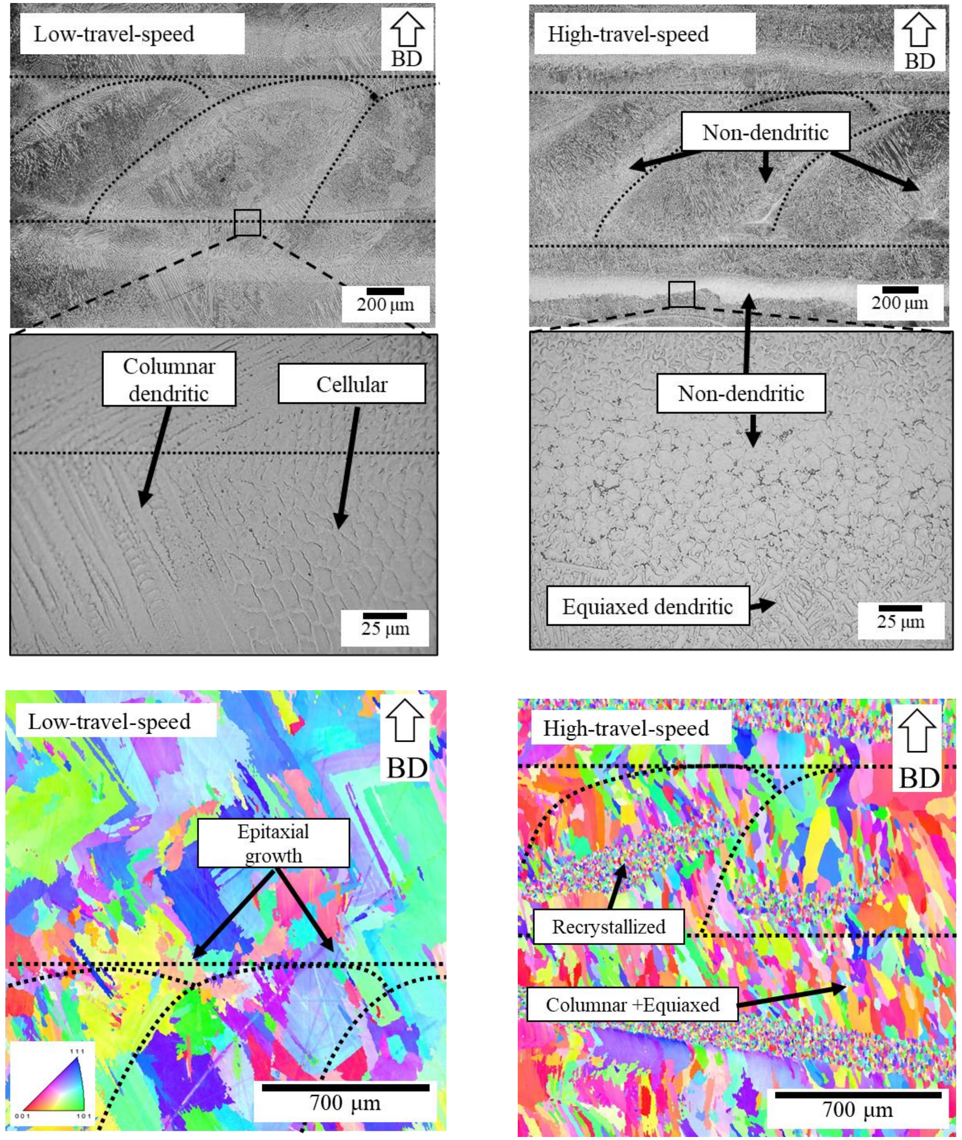

Preis et al., Influence of travel speed on microstructure and mechanical behavior of Inconel 625 fabricated using wire fed laser directed energy deposition (2024)

Influence of parameters on microstructure

- Solidification rate and thermal gradient calculated based on
  - Melt pool depth from thermal-fluid modeling
  - Melt pool length from thermal-fluid modeling
  - Cooling rate from experimental thermocouple data
- The high-travel-speed parameter has a lower thermal gradient and higher solidification rate.
- When plotted onto a microstructure selection chart, the calculated results are in agreement with experimental results.

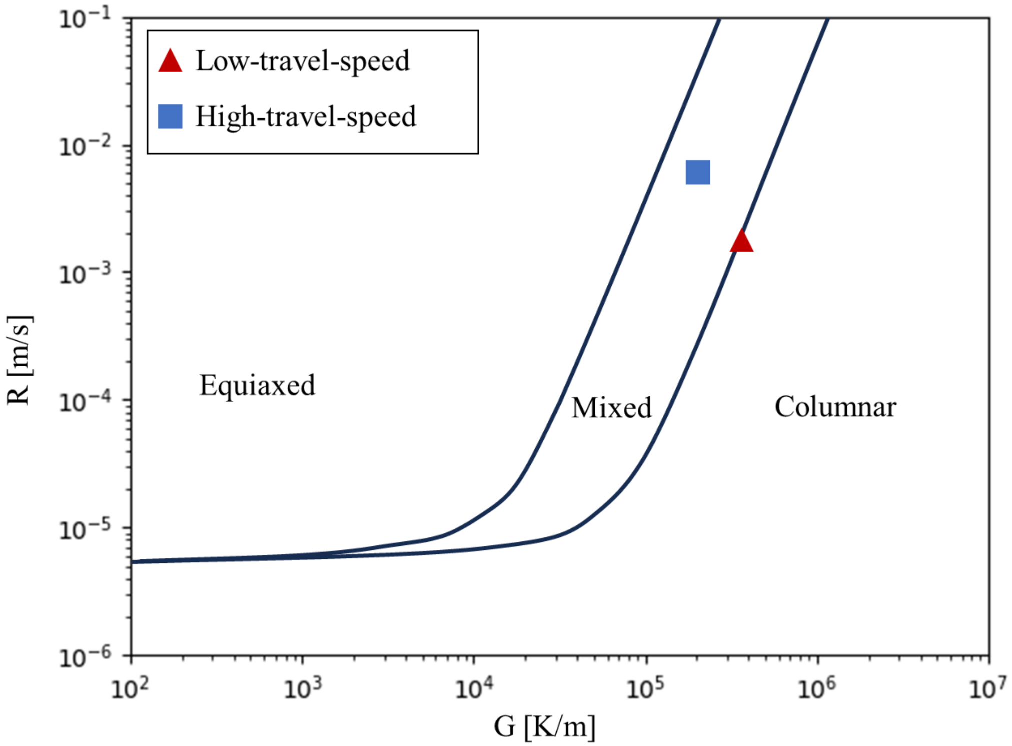

Parameter	Low-travel-speed	High-travel-speed
Melt pool depth [mm]	0.87	0.8
Melt pool length [mm]	2.81	2.17
Cooling rate [K/s]	723	1249
Solidification rate [m/s]	2.1×10^{-3}	6.2×10^{-3}
Thermal gradient [K/m]	3.5×10^{5}	2.0×10^{5}

Preis et al., Influence of travel speed on microstructure and mechanical behavior of Inconel 625 fabricated using wire fed laser directed energy deposition (2024)

Mechanical properties

- The high-travel-speed parameter shows a higher yield strength when pulled parallel to the build direction.
- Equivalent yield strength observed for both parameters when pulled perpendicular to the build direction.
- Higher yield strength observed for samples pulled perpendicular to the build direction.
- No difference in strain distribution observed between high travel speed and low travel speed parameters.

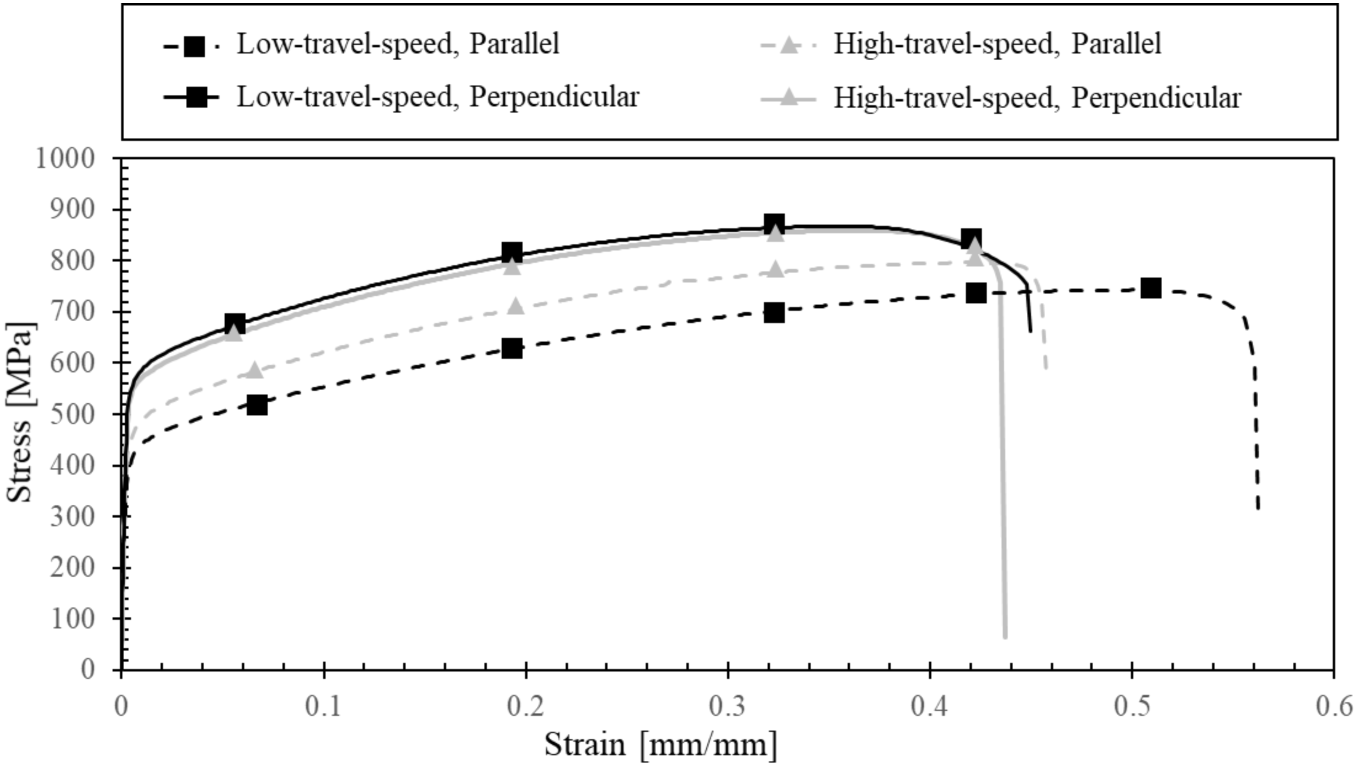

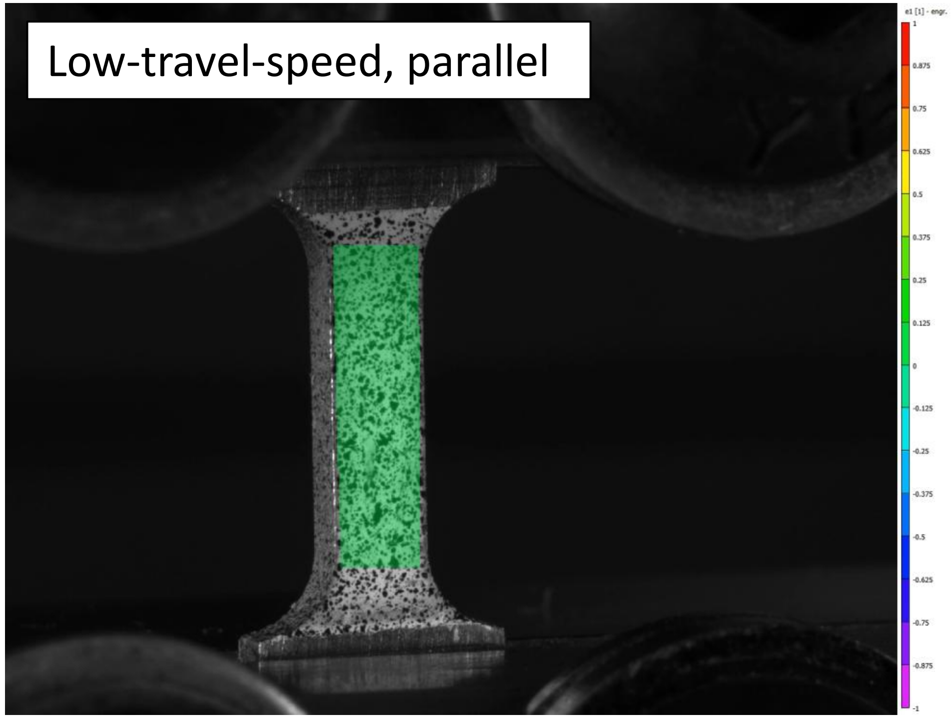

Preis et al., Influence of travel speed on microstructure and mechanical behavior of Inconel 625 fabricated using wire fed laser directed energy deposition (2024)

Influence of microstructure on mechanical properties

- Hall-Petch strengthening calculated for each parameter and orientation based on EBSD.
- Dislocation strengthening calculated for each parameter and orientation based on KAM (from EBSD).
- Results suggest dislocation strengthening primarily contributes to observed differences in yield strength.
- Calculations inaccurate for high-travel-speed due to non-isotropic structure
  - Cannot assume in-plane homogeneity.

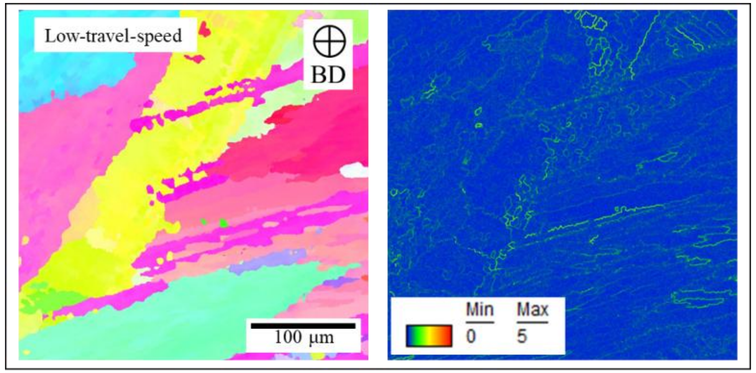

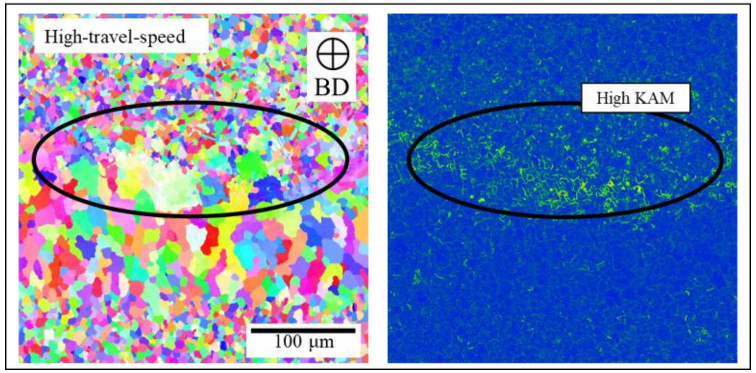

Orientation	Parameter	Hall-Petch strengthening *MPa*	Dislocation strengthening *MPa*	Total calculated *Mpa*	Experimental *MPa*
Parallel	Low-travel-speed	0	0	0	0
Perpendicular	Low-travel-speed	30	105	135	134
Parallel	High-travel-speed	27	52	79	45
Perpendicular	High-travel-speed	28	70	98	135

Preis et al., Influence of travel speed on microstructure and mechanical behavior of Inconel 625 fabricated using wire fed laser directed energy deposition (2024)

Outline

Goal: Understand the process-structure-property relationship in Inconel – GRCop42 joints

- Impact of parameters for LDED processing of wire Inconel 625
  - ❖ Manuscript 1: *Preis et al., Influence of travel speed on microstructure and mechanical behavior of Inconel 625 fabricated using wire fed laser directed energy deposition, Journal of Materials Processing Technology*

- Impact of Inconel 625 GRCop42 mixing
  - ❖ Manuscript 2: *Preis et al., Effect of Liquid Miscibility Gap on Defects in Inconel 625–GRCop42 Joints through Analysis of Gradient Composition Microstructure, Journal of Manufacturing and Materials Processing*

Inconel 625 GRCop42 mixtures

- Bimetallic joining of Inconel 625 with GRCop42 using LDED
  - ❖ Manuscript 3: *Preis et al., Effect of laser power and deposition sequence on microstructure of GRCop42 - Inconel 625 joints fabricated using laser directed energy deposition, Materials and Design*

- Development of a filler composition for joining of Inconel 718 with GRCop42 and LDED printing
  - ❖ Manuscript 4: *Microstructure, microhardness, and thermal properties of Inconel 718 - GRCop42 joint with liquid miscibility gap avoiding filler compositions*

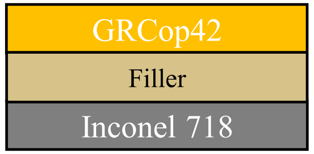

Key terms

- Liquid miscibility gap – two liquids cannot mix (lack of liquid state mixing).

Example: olive oil and balsamic vinaigrette

- Brittle phase – a composition and corresponding crystal structure which cannot withstand elongation.

Past work on Ni-superalloy GRCop joints

- Both **cracked** and **defect free** joints reported in the literature.
- No consensus as to the root cause and conditions under which cracking occurs – literature gap.

Cracked Joints

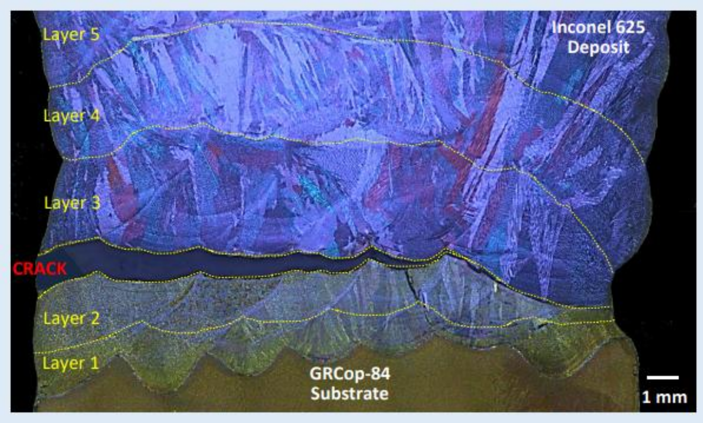

Wire Ebeam Inconel 625 onto GRCop84 [4]

Wire Ebeam Inconel 625 onto GRCop42 [5]

Defect Free Joints

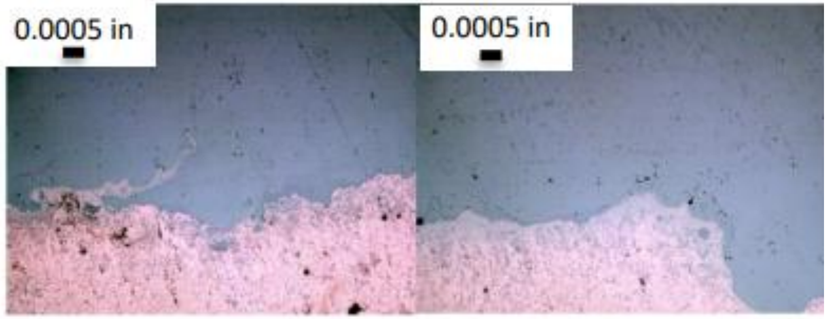

Powder DED onto GRCop42 [2]

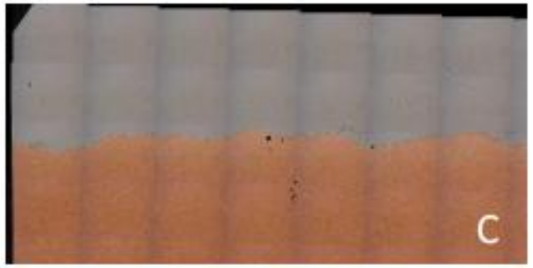

Wire EBeam onto GRCop84 [1]

[1] Progress in Additively Manufactured Copper-Alloy GRCop-84, GRCop-42, and Bimetallic Combustion Chambers for Liquid Rocket Engines
[2] Lightweight Thrust Chamber Assemblies using Multi-Alloy Additive Manufacturing and Composite Overwrap
[3]Characteristics of Bi-metallic Interfaces Formed During Direct Energy Deposition Additive Manufacturing Processing
[4] Electron Beam Freeform Fabrication of Dissimilar Materials: Cracking in Inconel® 625 Deposited on GRCop-84
[5] Advancing GRCop-based Bimetallic Additive Manufacturing to Optimize Component Design and Applications for Liquid Rocket Engines

Preis et al., Effect of Liquid Miscibility Gap on Defects in Inconel 625–GRCop42 Joints through Analysis of Gradient Composition Microstructure (2024)

Arc melting: mimicking melt pool mixing

- Arc melting is used to mimic the melt pool mixing without concerns of inhomogeneity and reheating that occurs in laser based processes.

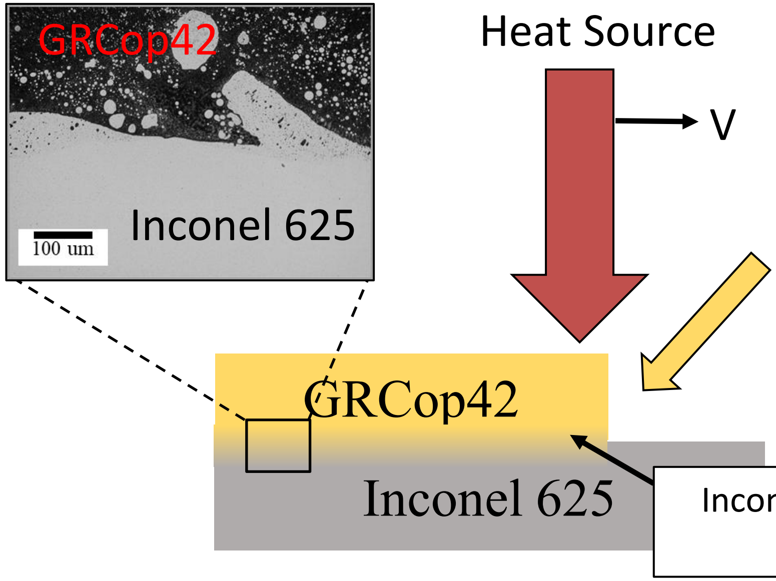

15 wt. % GRCop42
30 wt. % GRCop42
50 wt. % GRCop42
60 wt. % GRCop42
70 wt. % GRCop42
75 wt. % GRCop42
85 wt. % GRCop42
90 wt. % GRCop42
95 wt. % GRCop42

Edmund-Buhler AM200 Arc Melter

Optical Microscopy
XRD
EDS
Microhardness

Alloy	Ni	Cr	Nb	Ta	Mo	Cu	Fe	Ti	Al	Other
Inconel 625	**64.8**	**22.2**	**3.49**		**8.6**	.016	0.26	0.21	0.14	.284
GRCop42		**3.3**	**2.7**			***Bal***				

Preis et al., Effect of Liquid Miscibility Gap on Defects in Inconel 625–GRCop42 Joints through Analysis of Gradient Composition Microstructure (2024)

Microstructure of Inconel 625-GRCop42 Mixtures

- **Dendritic microstructure** observed in 15 wt. % GRCop42 sample

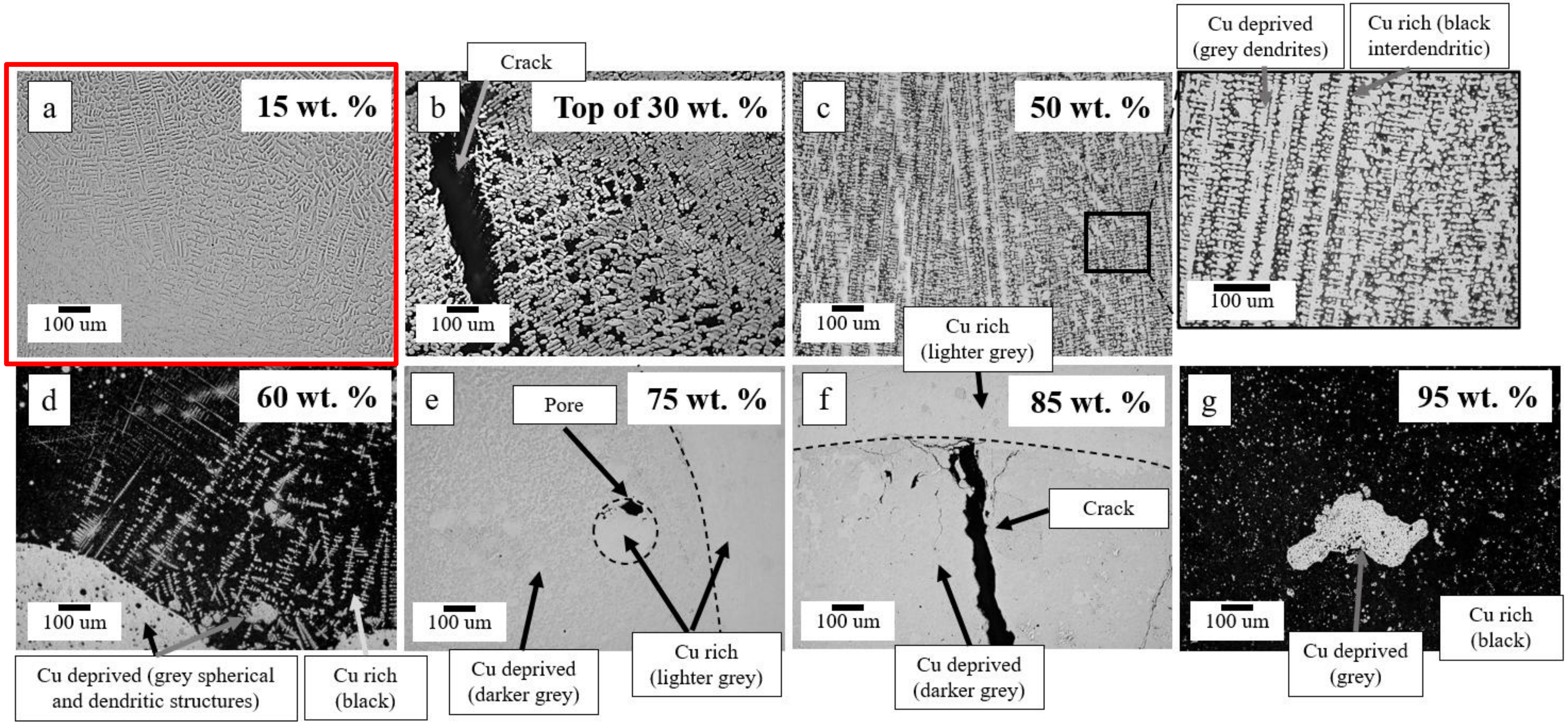

Preis et al., Effect of Liquid Miscibility Gap on Defects in Inconel 625–GRCop42 Joints through Analysis of Gradient Composition Microstructure (2024)

Microstructure of Inconel 625-GRCop42 Mixtures

- 30-50 wt. % GRCop42 samples show a **Cu-rich Cu-deprived dendritic morphology**

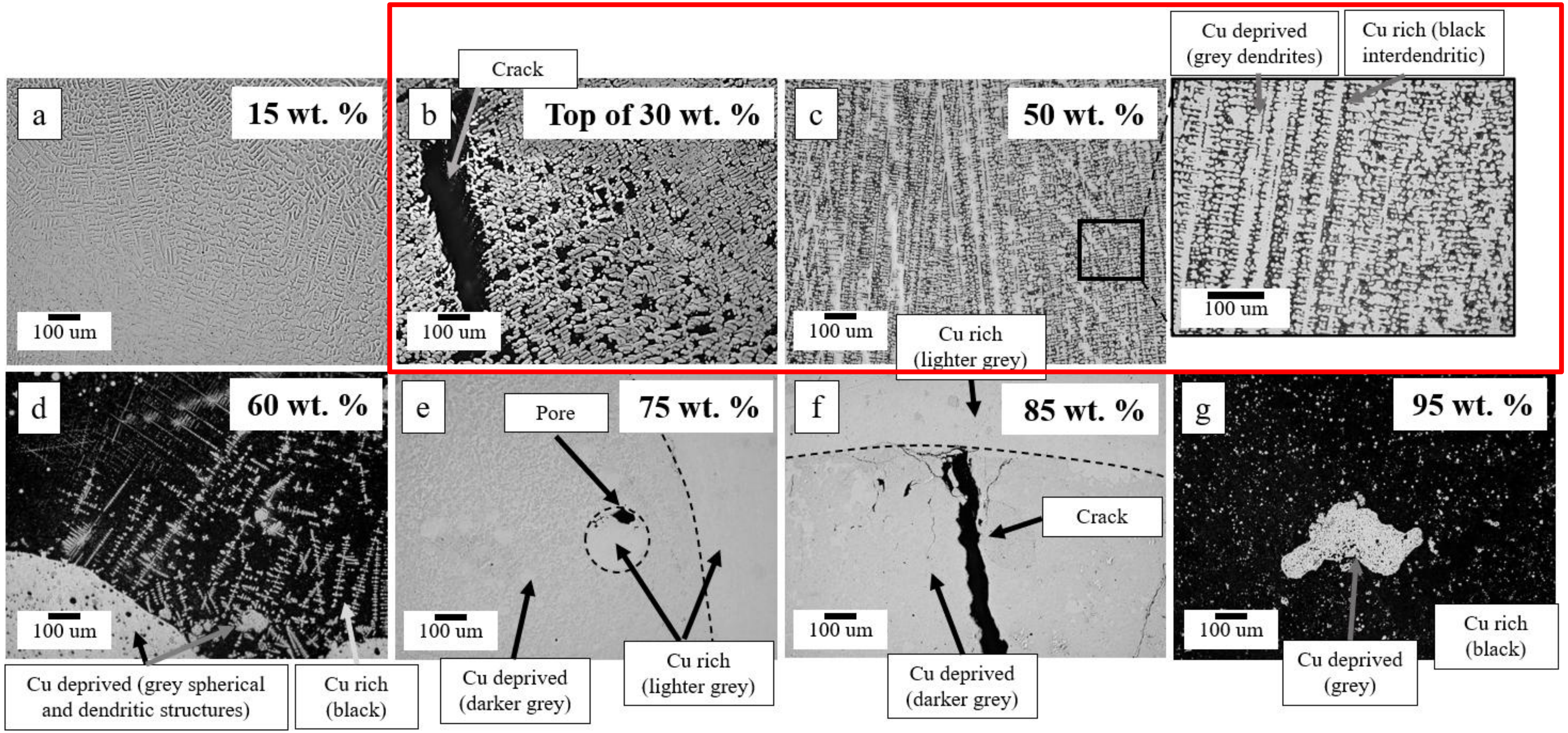

Preis et al., Effect of Liquid Miscibility Gap on Defects in Inconel 625–GRCop42 Joints through Analysis of Gradient Composition Microstructure (2024)

Microstructure of Inconel 625-GRCop42 Mixtures

- 60-95 wt. % GRCop42 samples show a **Cu-deprived spherical morphology.**

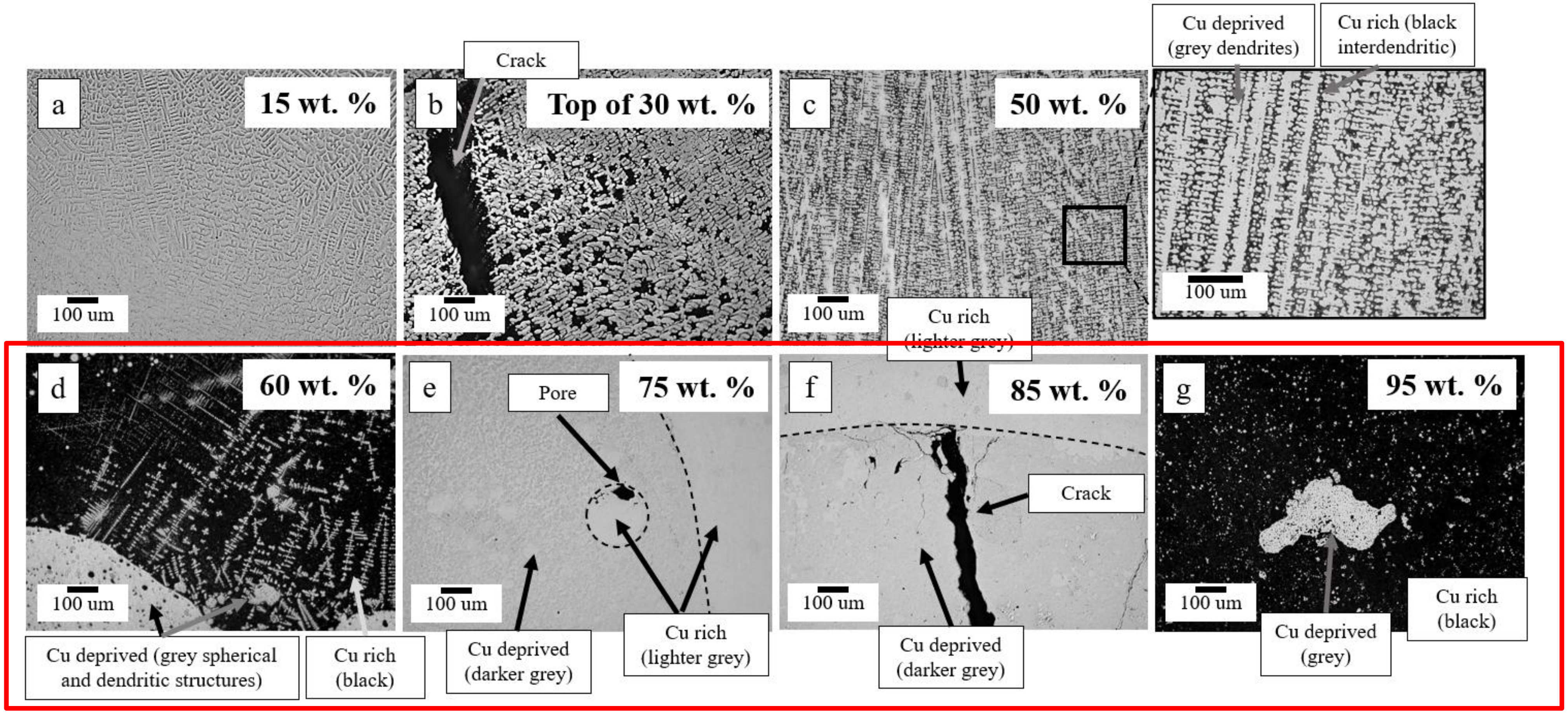

Preis et al., Effect of Liquid Miscibility Gap on Defects in Inconel 625–GRCop42 Joints through Analysis of Gradient Composition Microstructure (2024)

Oregon State University
College of Engineering

Liquid Miscibility Gap + Phase Analysis

Liquid Miscibility gap exists in Inconel 625-GRCop42

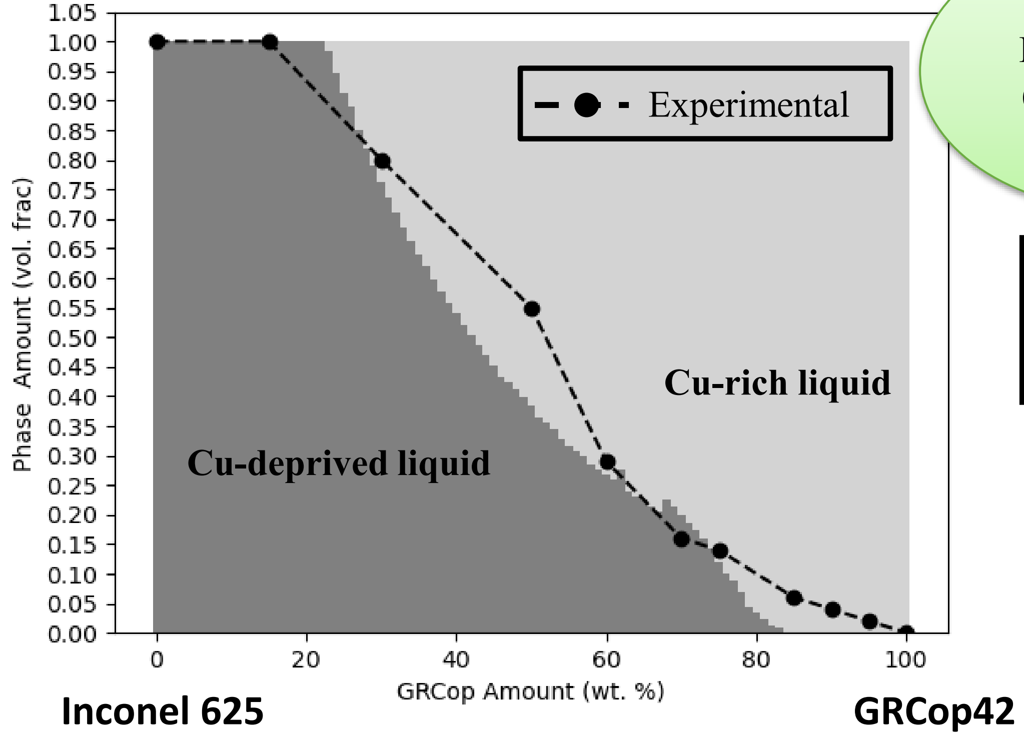

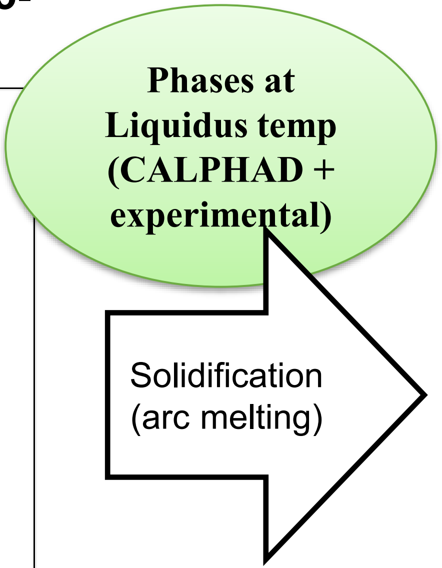

Brittle phase is formed from Cu-deprived liquid

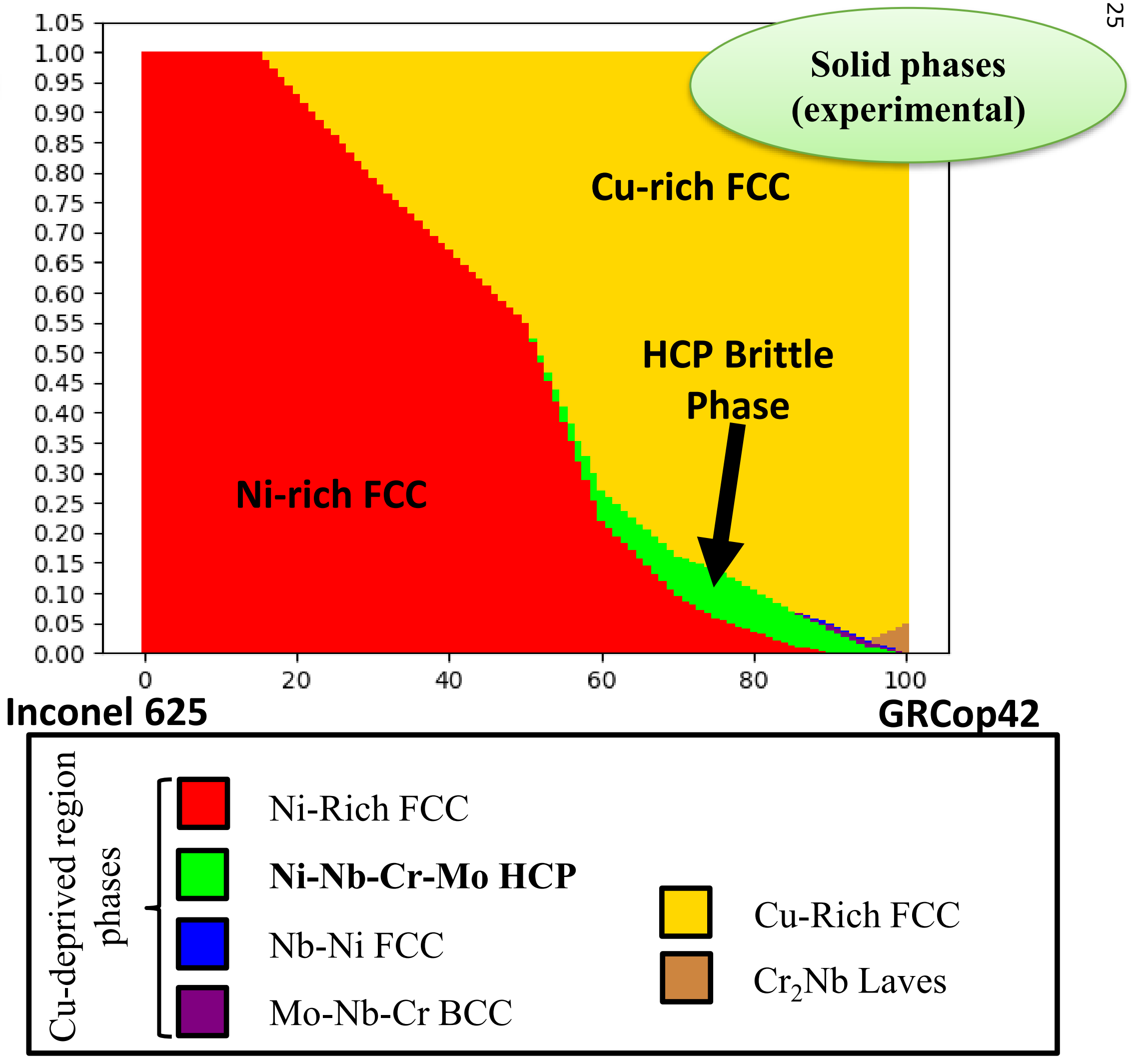

- Miscibility gap between Cu-rich and Cu-deprived liquid exists in Inconel 625 – GRCop42 phase diagram
- This miscibility gap results in brittle phase formation from the Cu-deprived liquid at compositions greater than 50 wt. % GRCop42

Preis et al., Effect of Liquid Miscibility Gap on Defects in Inconel 625–GRCop42 Joints through Analysis of Gradient Composition Microstructure (2024)

Identifying Defects in Mixing Inconel with GRCop

- Defects in GRCop42 – Inconel 625 mixtures are found to be compositionally dependent

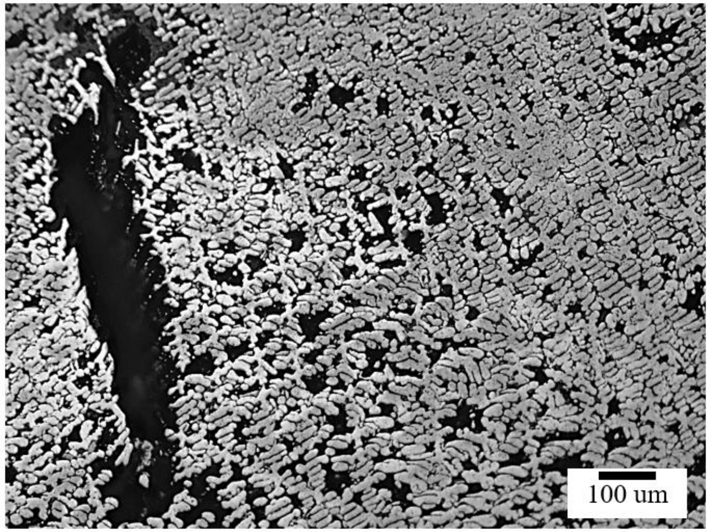

30-50 wt. % GRCop42

- Cracking observed at top 30 and 50 wt. % GRC samples
- These samples have a 2 phase dendritic microstructure

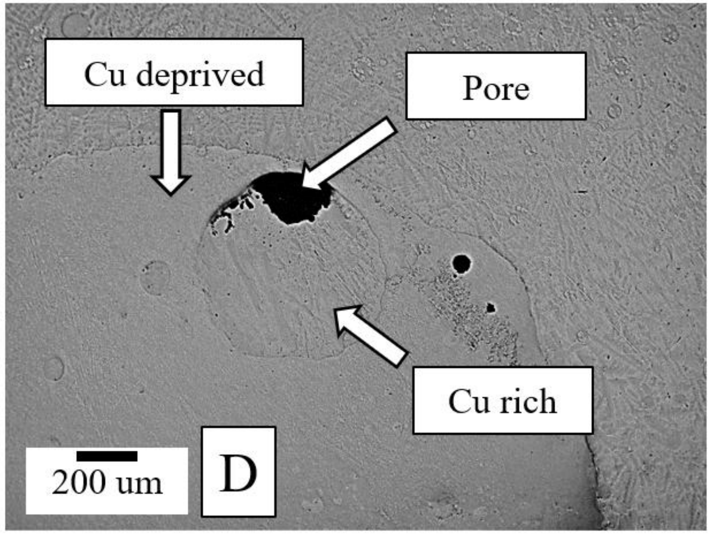

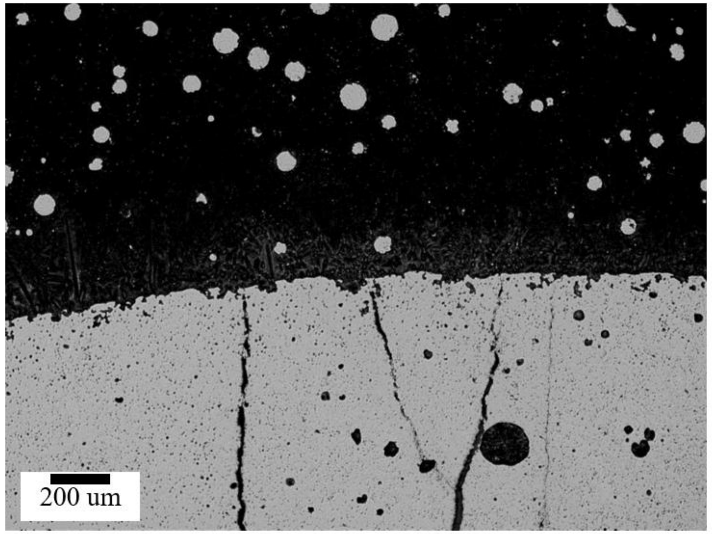

70 – 95 wt. % GRCop42

- Pores observed in the 70-95 wt. % GRC samples where Cu rich zones were trapped within Cu deprived zones.

- Cracking observed within the 70-95 wt. % Cu deprived zones.

Preis et al., Effect of Liquid Miscibility Gap on Defects in Inconel 625–GRCop42 Joints through Analysis of Gradient Composition Microstructure (2024)

Identifying Defects in Mixing Inconel with GRCop

- Defects in GRCop42 – Inconel 625 mixtures are found to be compositionally dependent

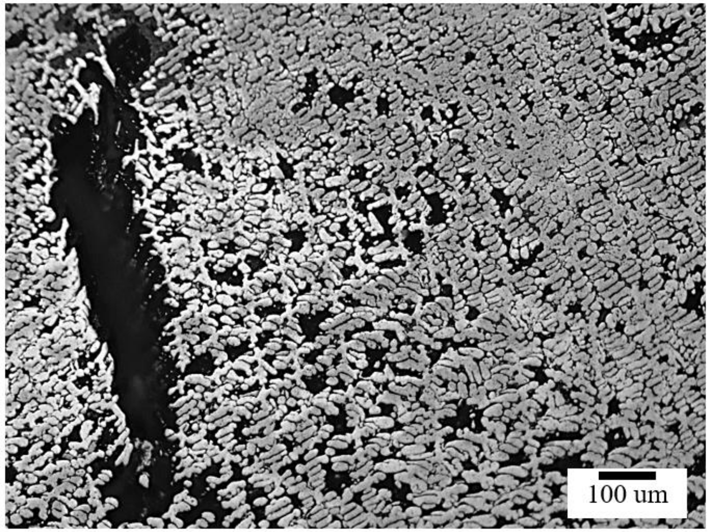

30-50 wt. % GRCop42

- Cracking observed at top 30 and 50 wt. % GRC samples
- These samples have a 2 phase dendritic microstructure

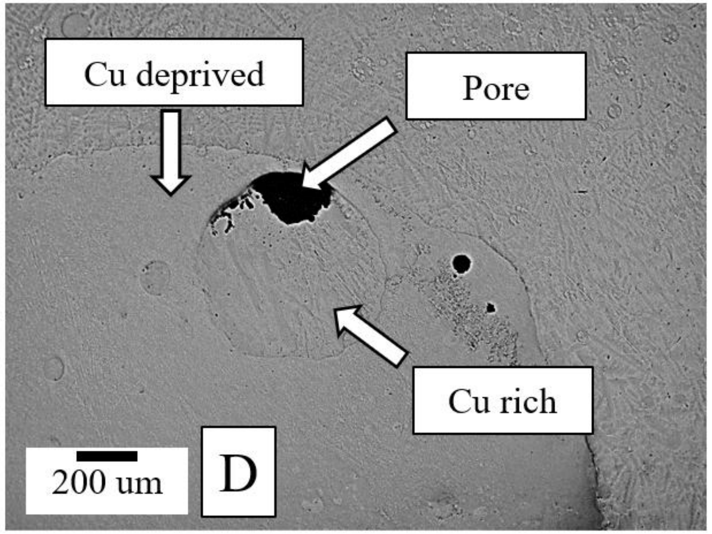

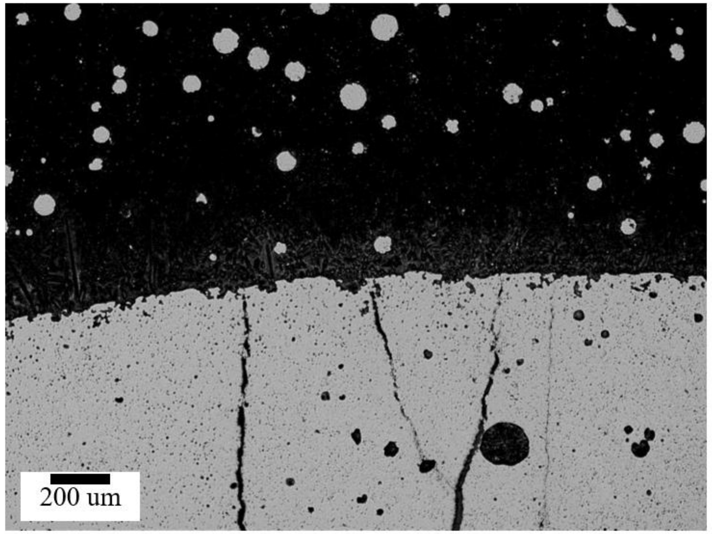

60 – 95 wt. % GRCop42

- Pores observed in the 70-95 wt. % GRC samples where Cu rich zones were trapped within Cu deprived zones.

- Cracking observed within the 70-95 wt. % Cu deprived zones.

Preis et al., Effect of Liquid Miscibility Gap on Defects in Inconel 625–GRCop42 Joints through Analysis of Gradient Composition Microstructure (2024)

Cracking Mechanism: Cu-Rich Liquid Entrapment

- Upon liquid separation due to the liquid miscibility gap, the Cu-deprived liquid solidifies first.
- This entraps the Cu-rich liquid, leading to Cu-rich liquid deficiency and cracking at the last point of solidification.
- This is a new cracking mechanism that has not been reported in literature.

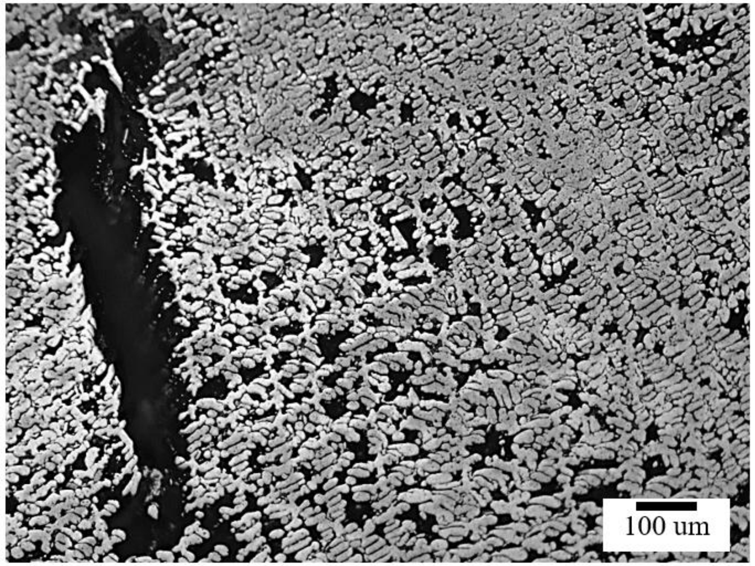

30 wt. % GRC

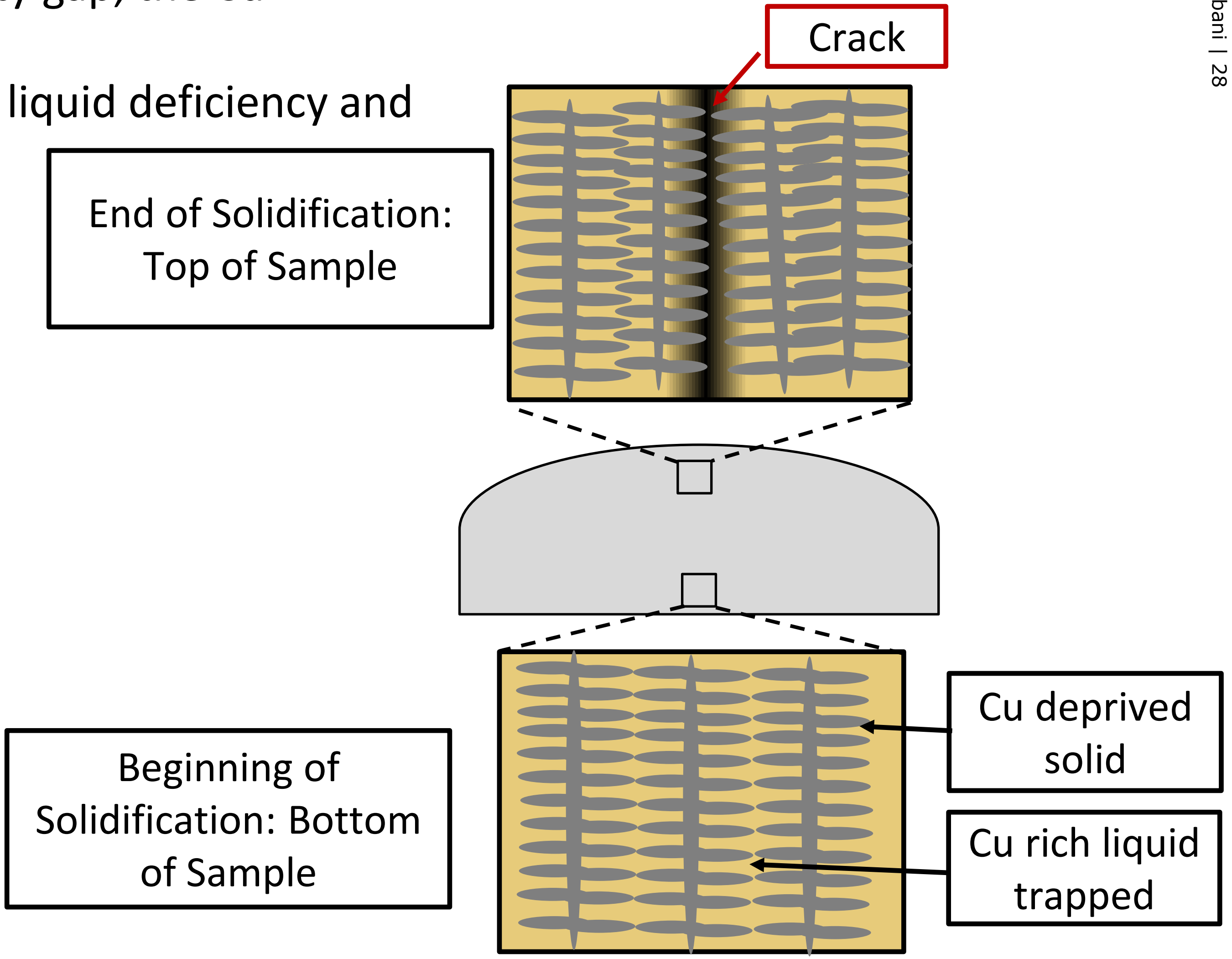

Preis et al., Effect of Liquid Miscibility Gap on Defects in Inconel 625–GRCop42 Joints through Analysis of Gradient Composition Microstructure (2024)

Identifying Defects in Mixing Inconel with GRCop

- Defects in GRCop42 – Inconel 625 mixtures are found to be compositionally dependent

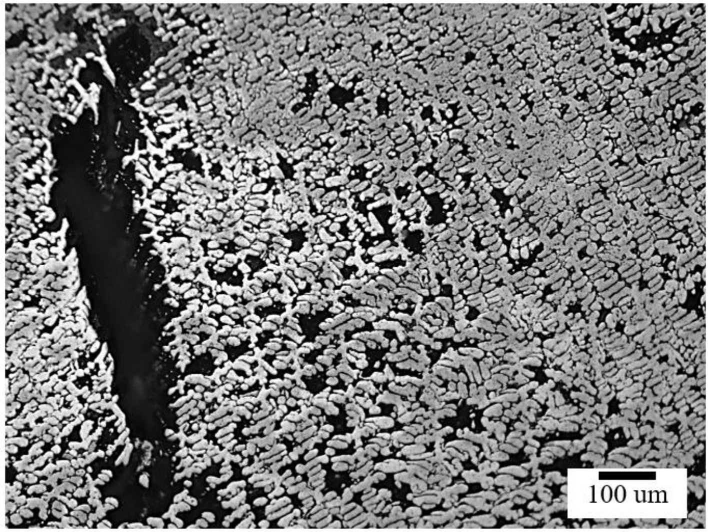

30-50 wt. % GRCop42

- Cracking observed at top 30 and 50 wt. % GRC samples
- These samples have a 2 phase dendritic microstructure

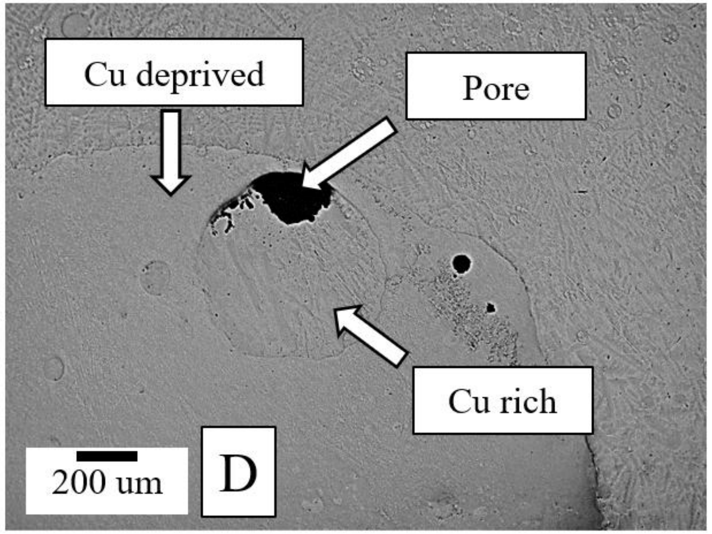

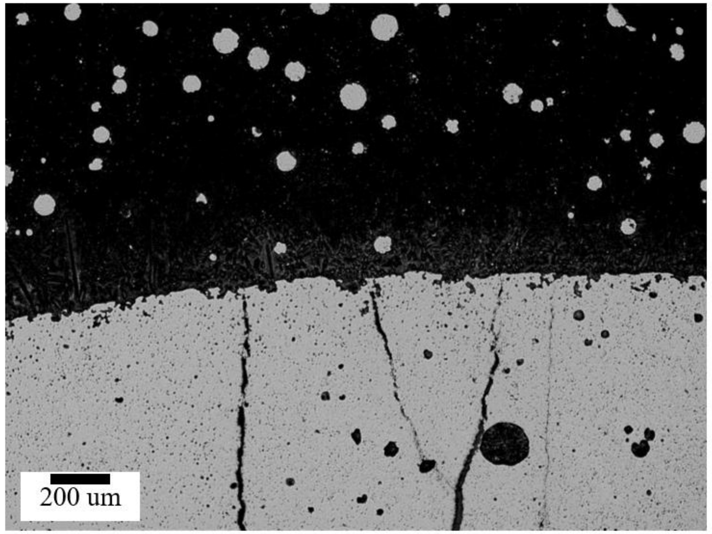

60 – 95 wt. % GRCop42

- Pores observed in the 70-95 wt. % GRC samples where Cu rich zones were trapped within Cu deprived zones.

- Cracking observed within the 70-95 wt. % Cu deprived zones.

Preis et al., Effect of Liquid Miscibility Gap on Defects in Inconel 625–GRCop42 Joints through Analysis of Gradient Composition Microstructure (2024)

Cracking Mechanism: Brittle Phase + Thermal Strain

- Upon solidification and cooling, high thermal gradients occur inducing thermal strain.
- The brittle phases in the Cu-deprived region of the 60-95 wt.% GRCop samples has high brittle phase volume fraction.
- The inability of the brittle phase to resolve thermal strain results in

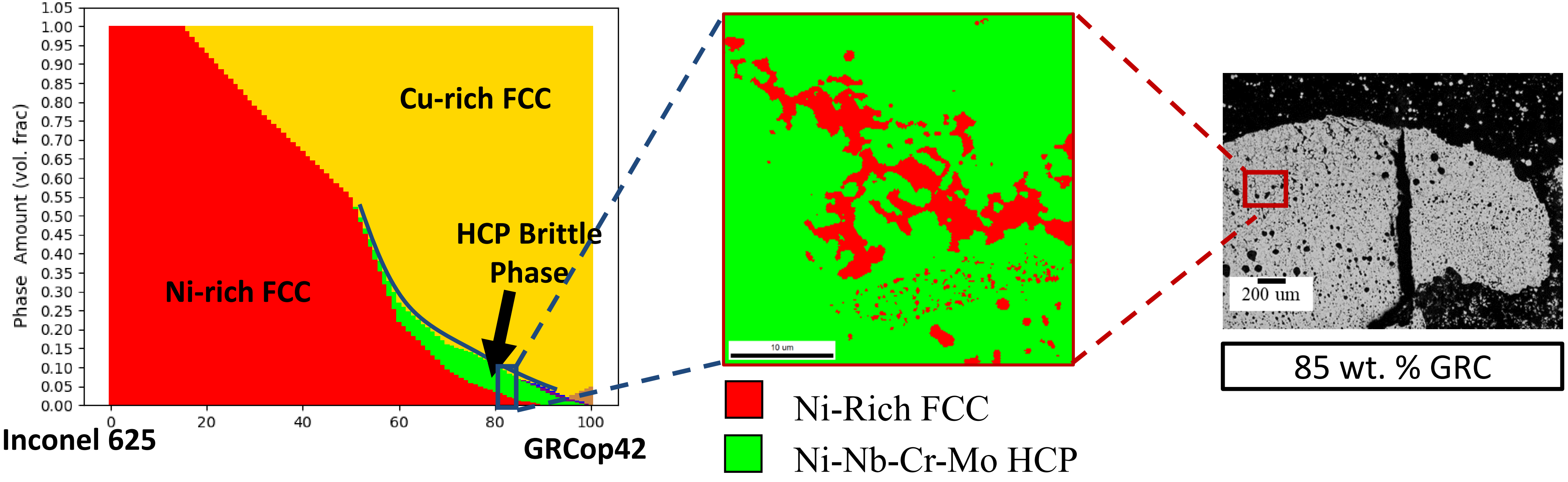

Preis et al., Effect of Liquid Miscibility Gap on Defects in Inconel 625–GRCop42 Joints through Analysis of Gradient Composition Microstructure (2024)

Validation of arc-melting to find defects in dissimilar metal AM

Arc melting | **LDED**

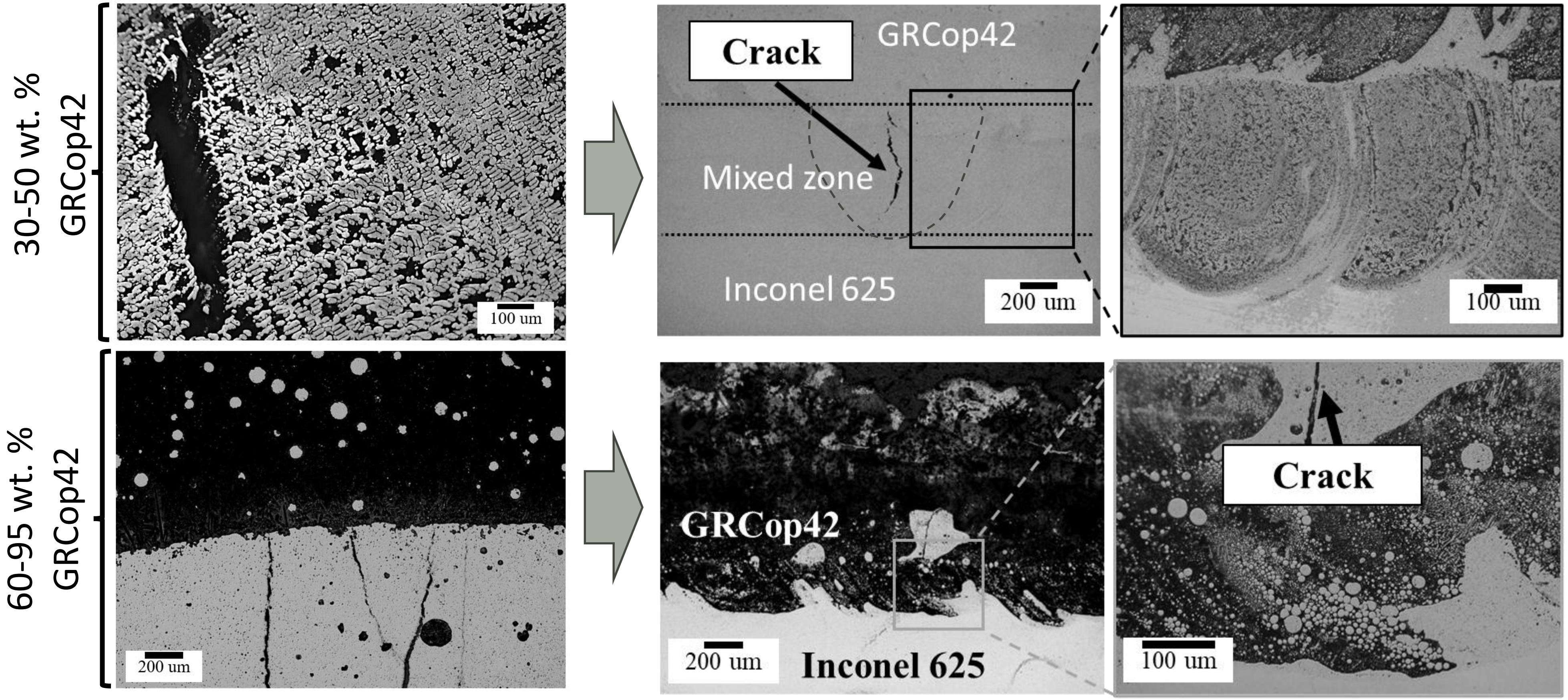

Higher remelting LDED parameter

- More Inconel 625 substrate remelted
- Cracking observed in middle of bead
- Morphology consistent with arc melting results

Lower remelting LDED parameter

- Less Inconel 625 substrate remelted
- Cu-deprived islands observed with cracks
- Morphology consistent with arc melting results

Preis et al., Effect of Liquid Miscibility Gap on Defects in Inconel 625–GRCop42 Joints through Analysis of Gradient Composition Microstructure (2024)

Summary

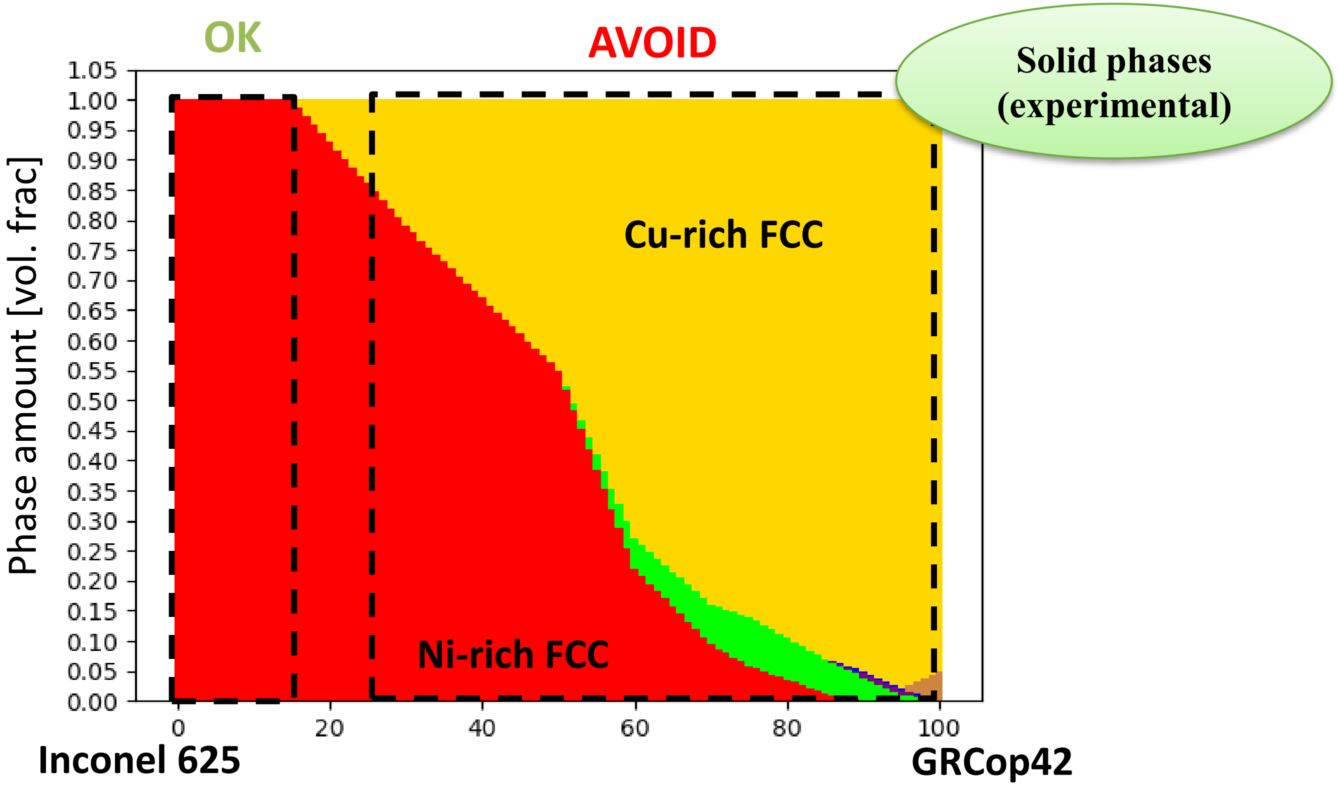
OK
AVOID
Solid phases
(experimental)
Phase amount [vol. frac]
1.05
1.00
0.95
0.90
0.85
0.80
0.75
0.70
0.65
0.60
0.55
0.50
0.45
0.40
0.35
0.30
0.25
0.20
0.15
0.10
0.05
0.00
Cu-rich FCC
Ni-rich FCC
0
20
40
60
80
100
Inconel 625
GRCop42

Outline

Goal: Understand the process-structure-property relationship in Inconel – GRCop42 joints

- Impact of parameters for LDED processing of wire Inconel 625
  - ❖ Manuscript 1: *Preis et al., Influence of travel speed on microstructure and mechanical behavior of Inconel 625 fabricated using wire fed laser directed energy deposition, Journal of Materials Processing Technology*

- Impact of Inconel 625 GRCop42 mixing
  - ❖ Manuscript 2: *Preis et al., Effect of Liquid Miscibility Gap on Defects in Inconel 625–GRCop42 Joints through Analysis of Gradient Composition Microstructure, Journal of Manufacturing and Materials Processing*

Inconel 625 GRCop42 mixtures

- Bimetallic joining of Inconel 625 with GRCop42 using LDED
  - ❖ Manuscript 3: *Preis et al., Effect of laser power and deposition sequence on microstructure of GRCop42 - Inconel 625 joints fabricated using laser directed energy deposition, Materials and Design*

- Development of a filler composition for joining of Inconel 718 with GRCop42 and LDED printing
  - ❖ Manuscript 4: *Microstructure, microhardness, and thermal properties of Inconel 718 - GRCop42 joint with liquid miscibility gap avoiding filler compositions*

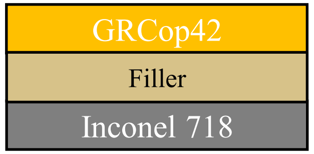

Key terms

- Melt pool – term used to describe the region of metal which is in the liquid state due to laser melting.

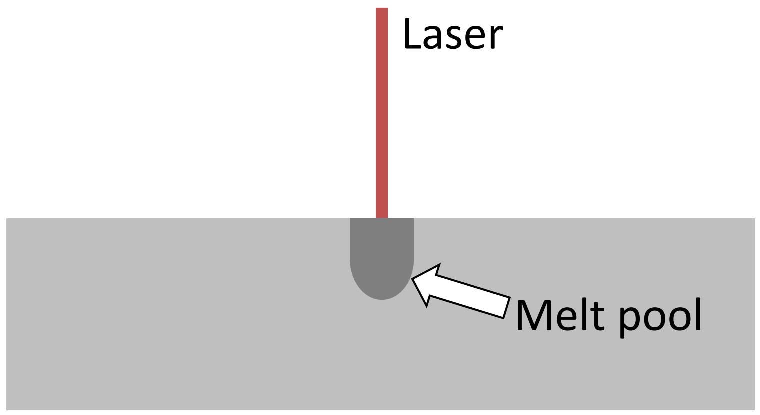

Inconel GRCop Bimetallic Joint via LDED

Joints Investigated

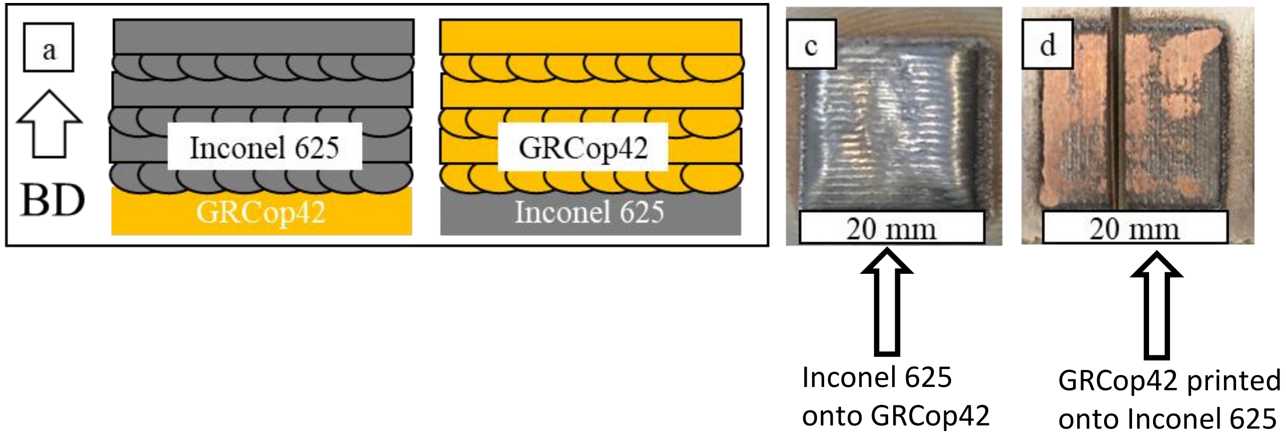

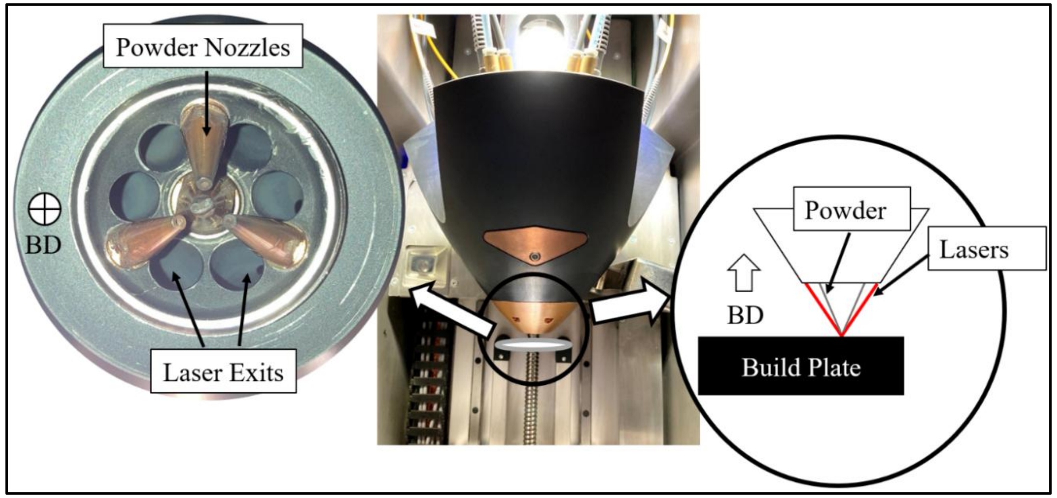

Materials

Alloy	Ni	Cr	Nb	Ta	Mo	Cu	Fe	Ti	Al	Other
Inconel 625 Wire	**64.8**	**22.2**	**3.49**		**8.6**	.016	0.26	0.21	0.14	.284
Inconel 625 Powder	*Bal*	**21.52**	**3.97**		**9.21**		0.85	0.4	0.24	.245
GRCop42		3.3	2.7			*Bal*				

- Meltio M450 system used for printing. Power was varied while travel speed was kept constant at **400 mm/min**. **2 g/min powder** feed rate was used for all prints.
- All top alloys were deposited using **powder directed energy deposition**.

Preis et al., Effect of Liquid Miscibility Gap on Defects in Inconel 625–GRCop42 Joints through Analysis of Gradient Composition Microstructure (2024)

Inconel GRCop Bimetallic Joint via LDED

Joints Investigated

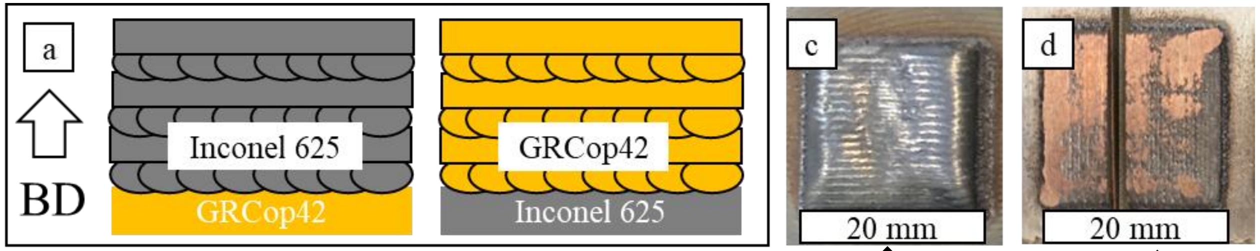

Inconel 625 onto GRCop42

GRCop42 printed onto Inconel 625

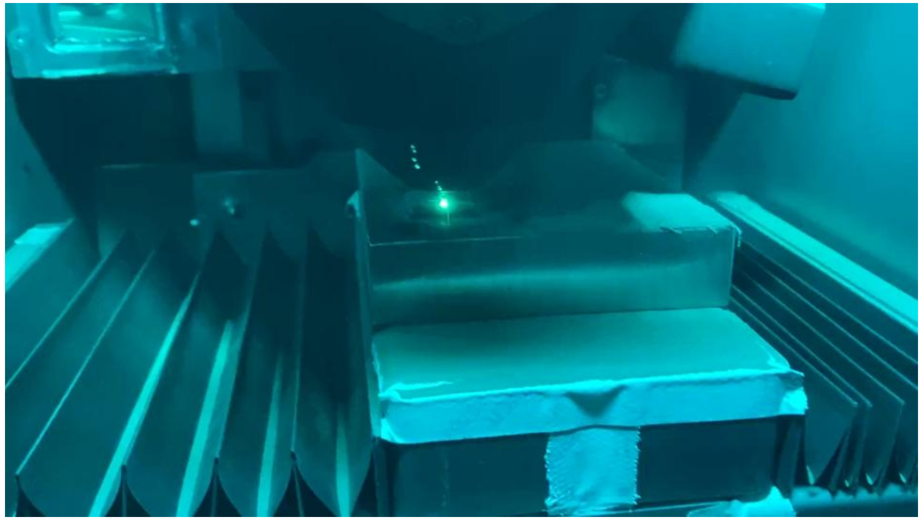

Materials

Alloy	Ni	Cr	Nb	Ta	Mo	Cu	Fe	Ti	Al	Other
Inconel 625 Wire	**64.8**	**22.2**	**3.49**		**8.6**	.016	0.26	0.21	0.14	.284
Inconel 625 Powder	*Bal*	**21.52**	**3.97**		**9.21**		0.85	0.4	0.24	.245
GRCop42		3.3	2.7			*Bal*				

- Meltio M450 system used for printing. Power was varied while travel speed was kept constant at **400 mm/min**. **2 g/min powder** feed rate was used for all prints.
- All top alloys were deposited using **powder directed energy deposition**.

Preis et al., Effect of Liquid Miscibility Gap on Defects in Inconel 625–GRCop42 Joints through Analysis of Gradient Composition Microstructure (2024)

Inconel 625 onto GRCop42

- When depositing Inconel 625 onto GRCop42 at 600 W, lack of fusion observed in the first layer due to the GRCop42 acting as a heat sink.
- The lack of fusion is avoided by increasing the laser power in the first layer.
- Defect-free joint achieved – miscibility gap avoided.

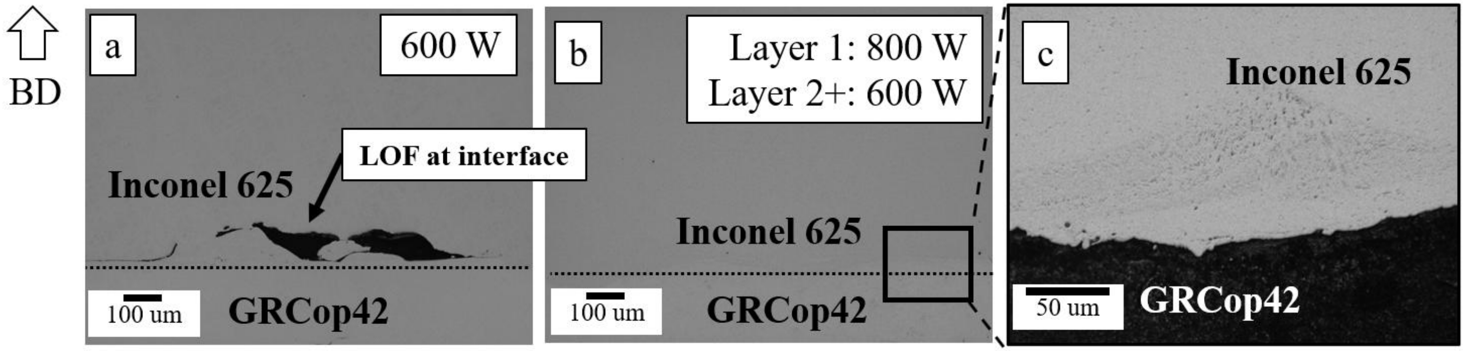

800 W, 400 mm/min onto GRCop42

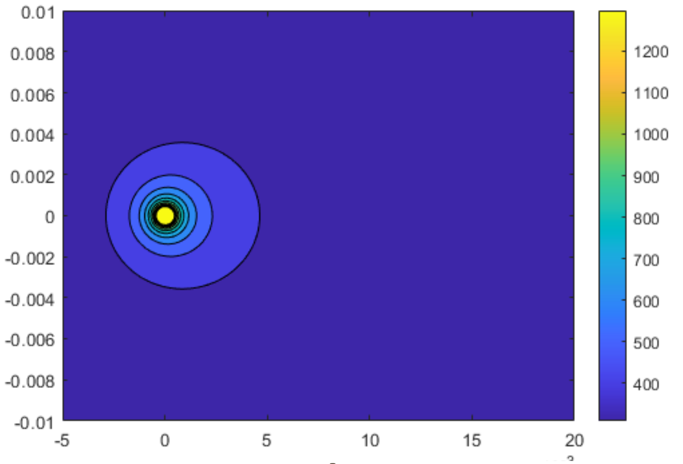

800 W, 400 mm/min onto Inconel 625

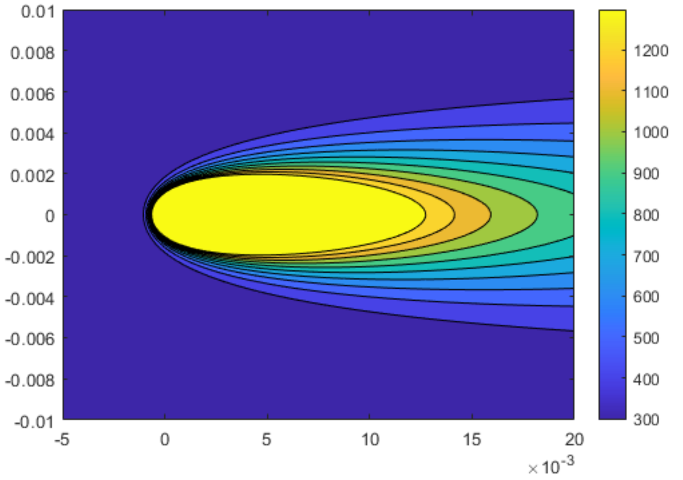

Preis et al., Effect of Liquid Miscibility Gap on Defects in Inconel 625–GRCop42 Joints through Analysis of Gradient Composition Microstructure (2024)

Inconel 625 onto GRCop42

- When depositing Inconel 625 onto GRCop42 at 600 W, lack of fusion observed in the first layer due to the GRCop42 acting as a heat sink.
- The lack of fusion is avoided by increasing the laser power in the first layer.
- Defect-free joint achieved – miscibility gap avoided by remelting less than 20 wt.% GRCop42.

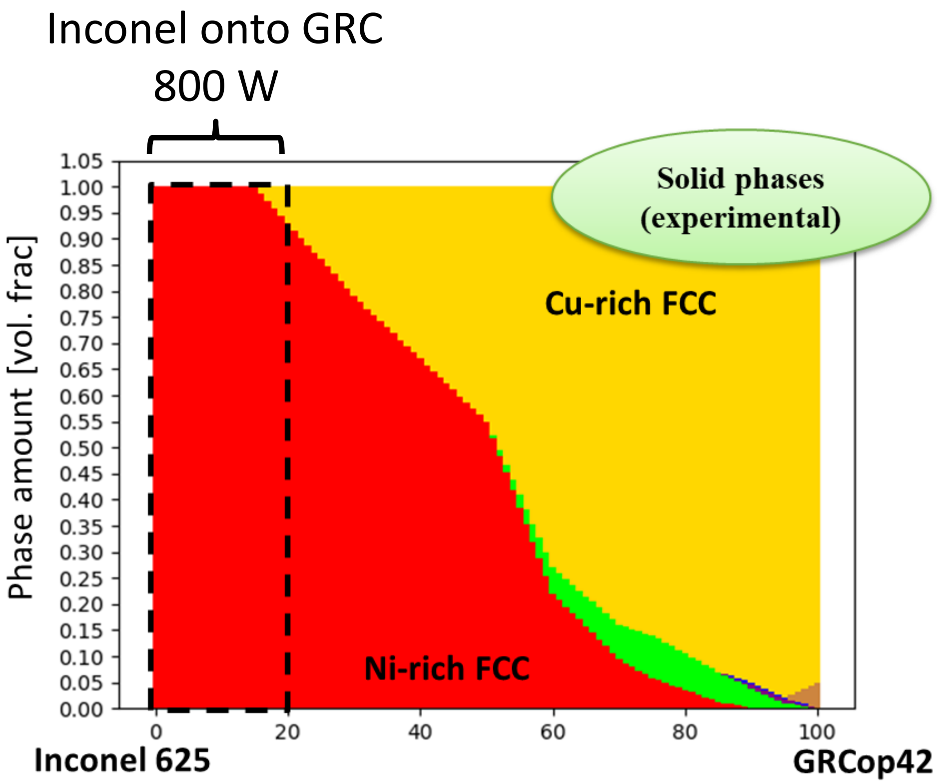

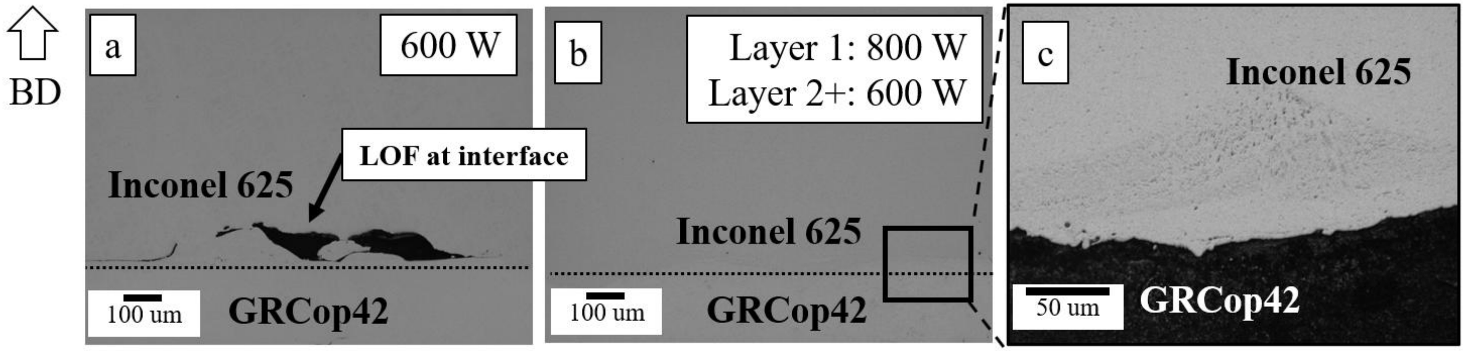

Preis et al., Effect of Liquid Miscibility Gap on Defects in Inconel 625–GRCop42 Joints through Analysis of Gradient Composition Microstructure (2024)

GRCop42 onto Inconel 625

- **Islands** and **peninsulas** observed above the Inconel 625 GRCop42 interface.
- Presence of **islands** and **peninsulas** can be explained by presence of liquid miscibility gap.
- **Cracks** present in islands of 400 W sample.

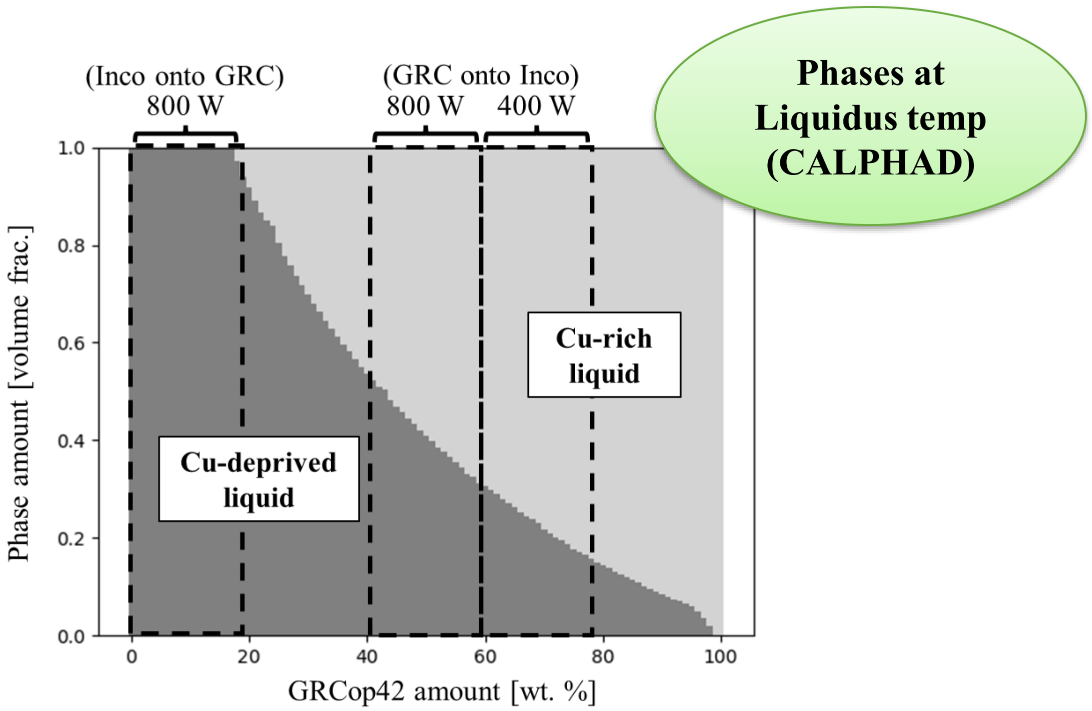

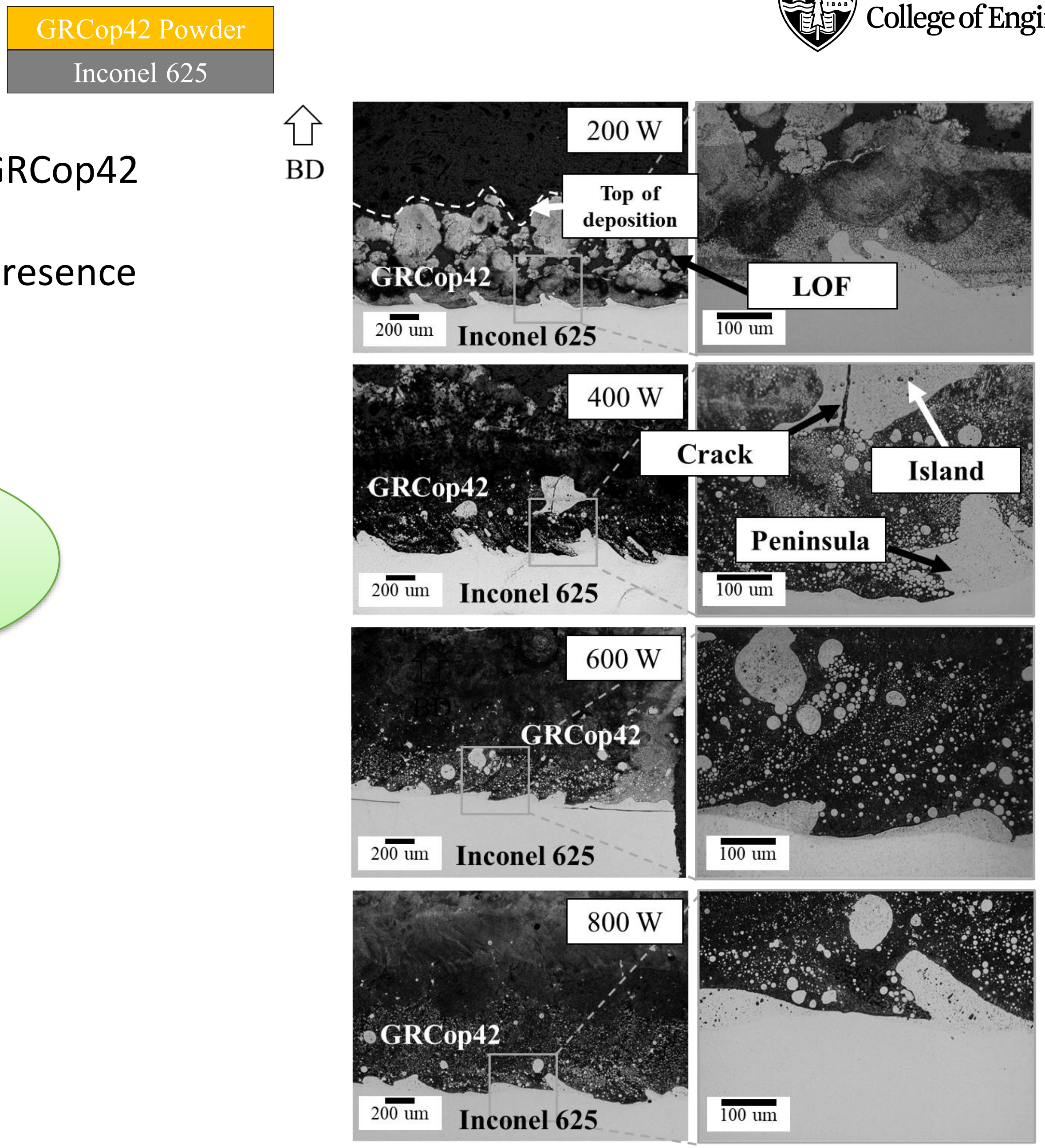

Preis et al., Effect of Liquid Miscibility Gap on Defects in Inconel 625–GRCop42 Joints through Analysis of Gradient Composition Microstructure (2024)

GRCop42 onto Inconel 625

- High microhardness Cu-deprived islands and peninsulas observed.
- Cracks present in islands of 400 W sample.
- By increasing laser power, the amount of remelting of GRCop42 with Inconel 625 was increased, creating islands with a lower hardness / lower brittle phase volume fraction.

Increased power results in fewer brittle phases, but *<u>does not</u>* eliminate them

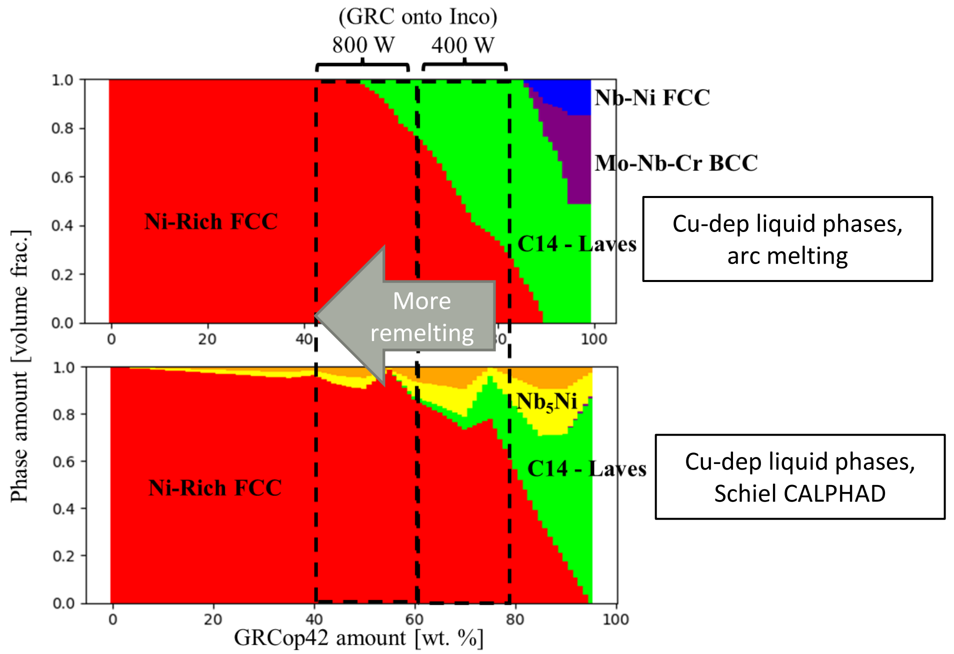

Sample	Peninsula *HV.5*	Island *HV.5*
400 W	382 ± 75	718 ± 159
600 W	400 ± 105	665 ± 216
800 W	401 ± 134	590 ± 215
GRCop42	114 ± 28	
Inconel 625	262 ± 27	

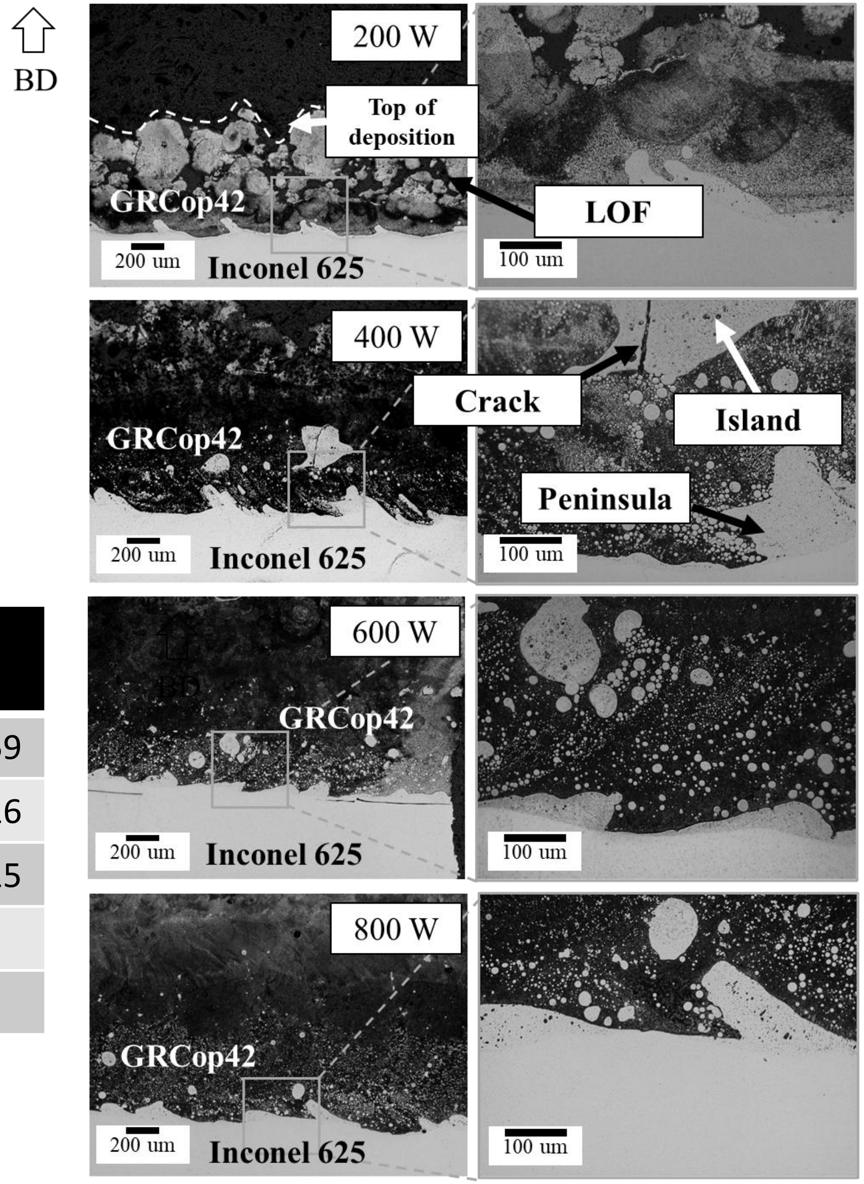

Preis et al., Effect of Liquid Miscibility Gap on Defects in Inconel 625–GRCop42 Joints through Analysis of Gradient Composition Microstructure (2024)

Summary

NO BRITTLE PHASE FORMATION / CRACKING

CRACKING IN ISLANDS DUE TO BRITTLE PHASES

Outline

Goal: Understand the process-structure-property relationship in Inconel – GRCop42 joints

- Impact of parameters for LDED processing of wire Inconel 625
  - ❖ Manuscript 1: *Preis et al., Influence of travel speed on microstructure and mechanical behavior of Inconel 625 fabricated using wire fed laser directed energy deposition, Journal of Materials Processing Technology*

- Impact of Inconel 625 GRCop42 mixing
  - ❖ Manuscript 2: *Preis et al., Effect of Liquid Miscibility Gap on Defects in Inconel 625–GRCop42 Joints through Analysis of Gradient Composition Microstructure, Journal of Manufacturing and Materials Processing*

Inconel 625 GRCop42 mixtures

- Bimetallic joining of Inconel 625 with GRCop42 using LDED
  - ❖ Manuscript 3: *Preis et al., Effect of laser power and deposition sequence on microstructure of GRCop42 - Inconel 625 joints fabricated using laser directed energy deposition, Materials and Design*

- Development of a filler composition for joining of Inconel 718 with GRCop42 and LDED printing
  - ❖ Manuscript 4: *Microstructure, microhardness, and thermal properties of Inconel 718 - GRCop42 joint with liquid miscibility gap avoiding filler compositions*

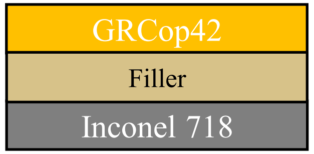

Developing transition compositions

- Inconel 718 is a Ni-based superalloy similar to Inconel 625.
- Goal: develop and fabricate a GRCop42 Inconel 718 joint which avoids the brittle phase formation by use of developed transition compositions.

Material	Use	Ni	Cr	Nb	Mo	Cu	Fe	Al	Other
Inconel 718 Wire	*AM, P*	52.3	17.94	5.1	2.96	-	18.74	0.49	-
Ni Wire	*AM*	99.6	-	-	-	<0.01	0.17	-	0.2
Cu Wire	*AM*	-	-	-	-	99.9	-	-	0.1
Ni Powder	*P*	99.9	-	-	-	<0.01	<0.01	-	-
Cu Powder	*P*	-	-	-	-	99.95	-	-	0.05
GRCop42 Powder	*AM,P*	-	3.3	2.7	-	Bal	-	-	-

AM for materials used in arc melting, P for materials used for printing

CALPHAD → Arc melting → LDED printing → Characterization

Identify transition compositions | *Validate CALPHAD* | *Fabricate joint with transition compositions* | *Microstructure and microhardness of joint*

GRCop42 ⇕ Cu – based transition ⇕ Ni – based transition ⇕ Inconel 718

CALPHAD Predictions

- Methodology: Use Cu and Ni based filler composition.
  - Cu is fully soluble with GRCop42
  - Ni if fully soluble with Cu
  - Ni is fully soluble with Inconel 718.
- Brittle phases predicted at regions with high wt. % of GRCop42.

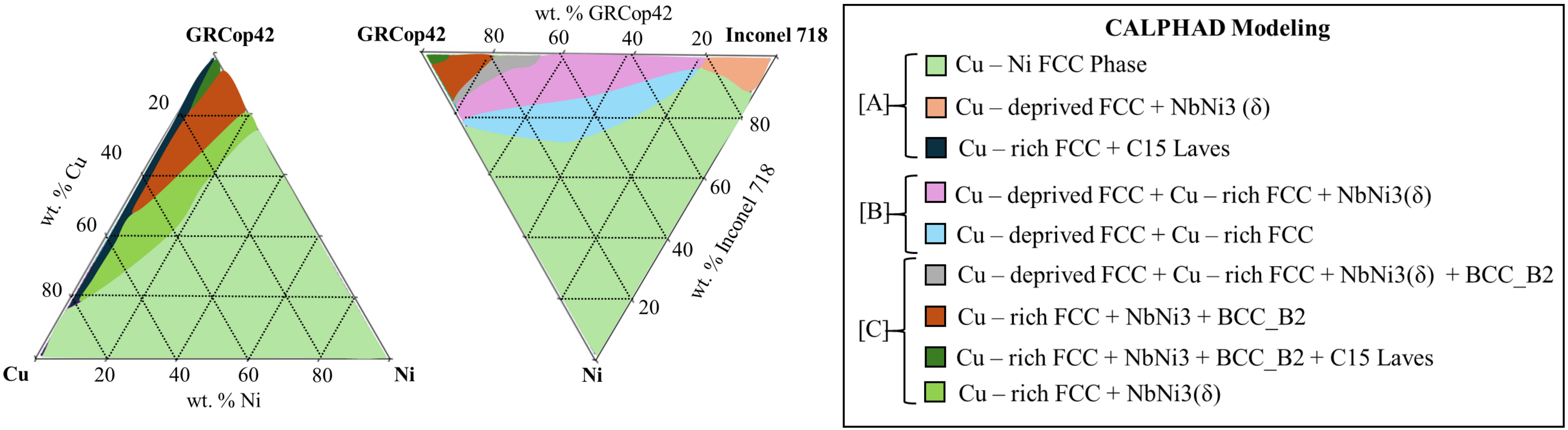

CALPHAD Predictions

- Methodology: Use Cu and Ni based filler composition.
  - Cu is fully soluble with GRCop42
  - Ni if fully soluble with Cu
  - Ni is fully soluble with Inconel 718.
- Brittle phases predicted at regions with high wt. % of GRCop42.

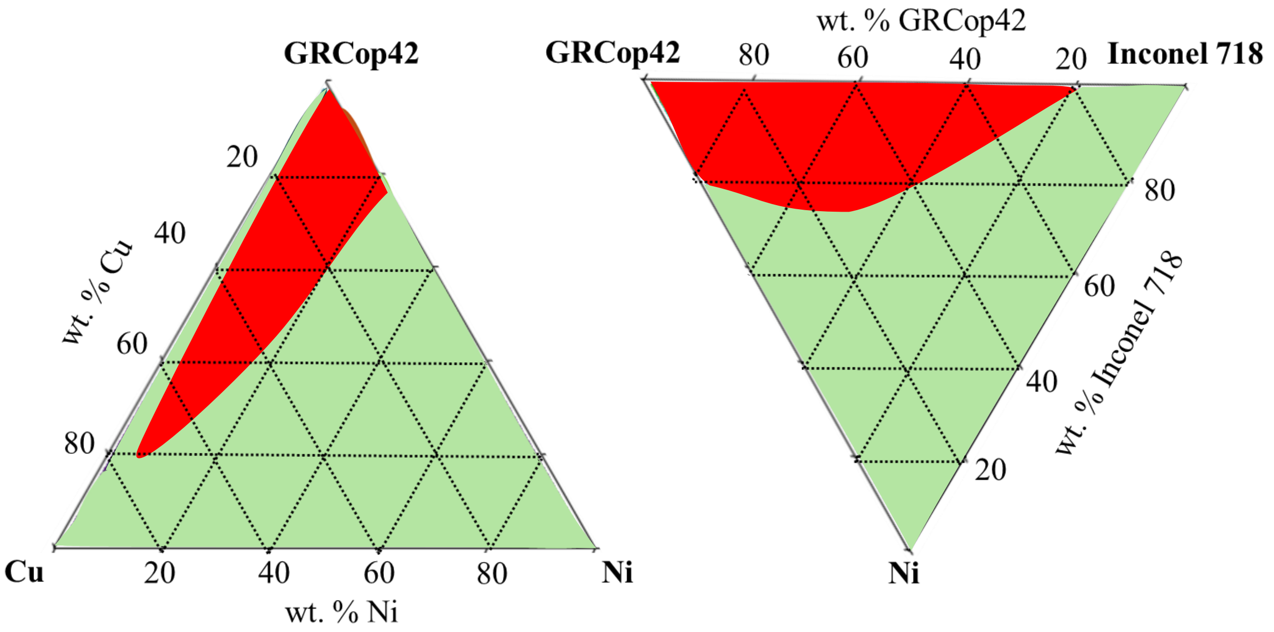

Brittle phase formation + liquid miscibility gap (avoid)

No brittle phase formation and liquid miscibility gap

Arc melted samples

- Arc melted samples confirm “no go” region for joining Inconel 718 and GRCop42.

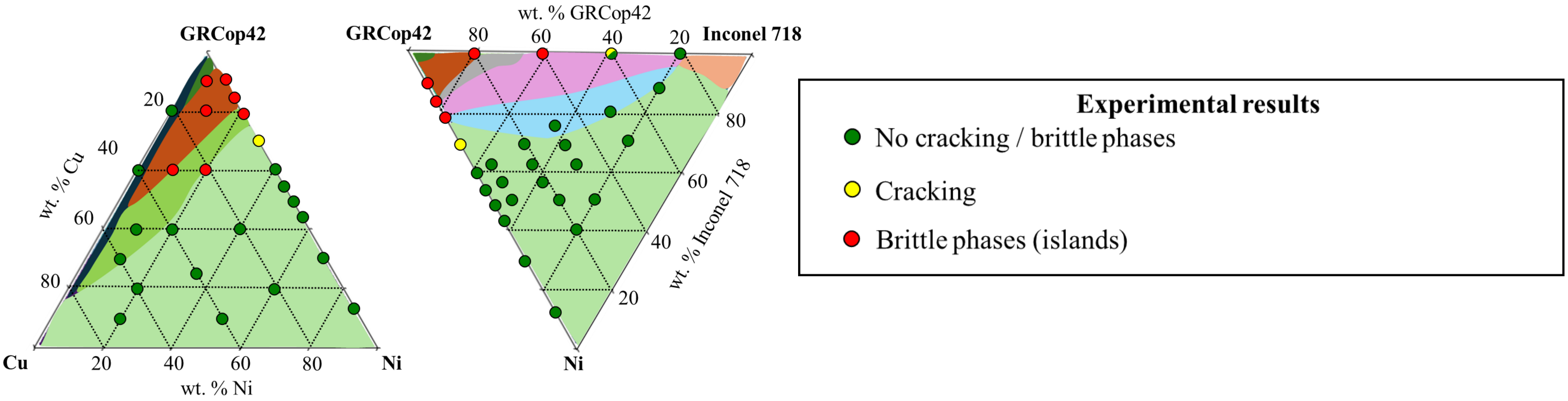

Criterion for choosing transition compositions

1. Avoid regions with brittle phase formation.
2. Avoid regions of low strength.
3. Chose as few transition compositions as possible.

CALPHAD + Arc melted samples

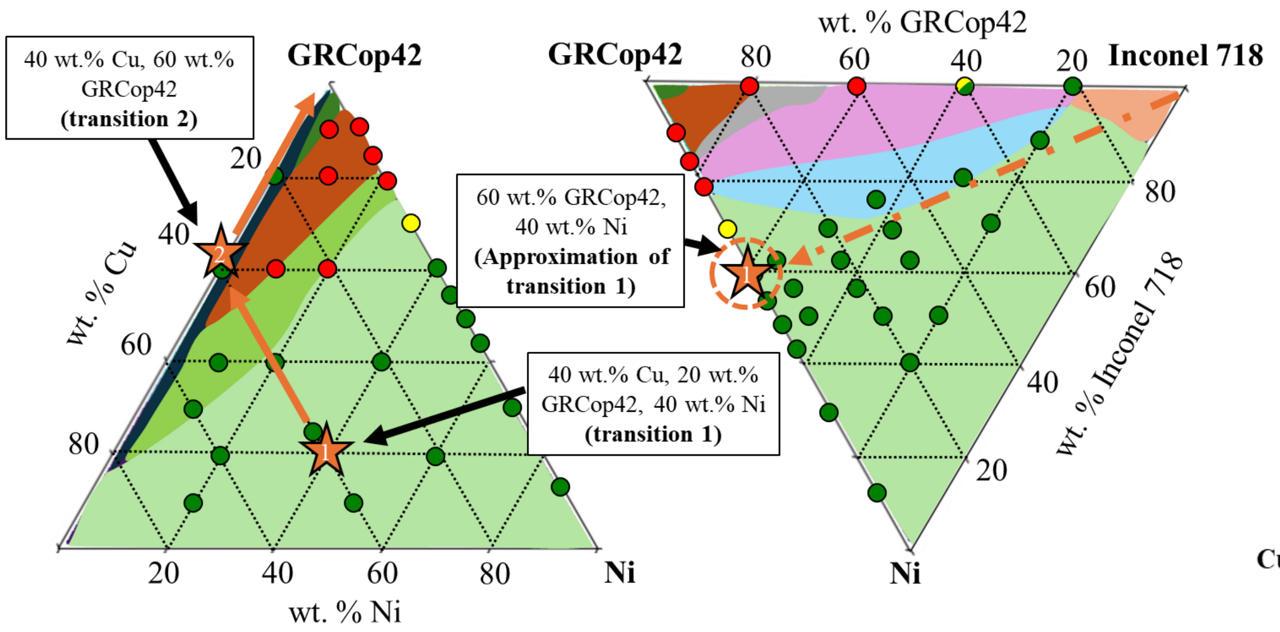

Experimental microhardness results for mechanical property prediction

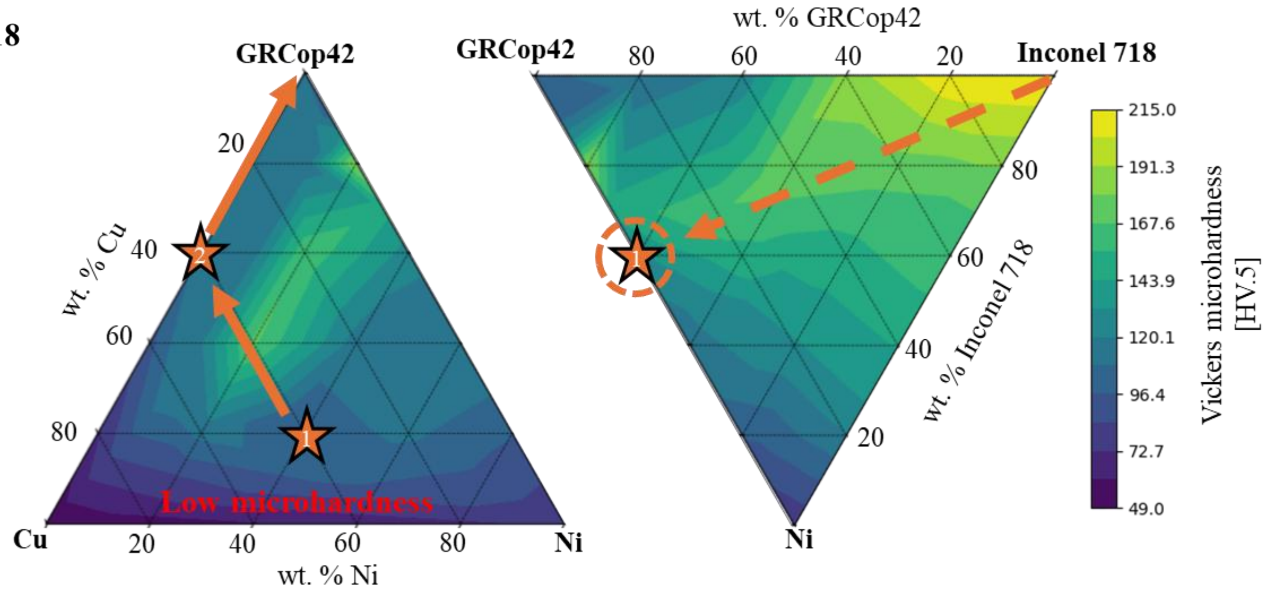

Printing the joint

- Transition compositions created for LDED by mechanical mixing Cu, Ni, and GRCop42 power.
  - Transition 1: 20 wt.% GRCop42, 40 wt.% Ni, 40 wt.% Ni
  - Transition 2: 60 wt.% GRCop42, 40 wt.% Cu
- Joint printed on Meltio M450
- Parameters adjusted in-situ for avoidance of defects.
- Speed of 400 mm/min and powder feed rate of 2 g/min was used for all powder printing.

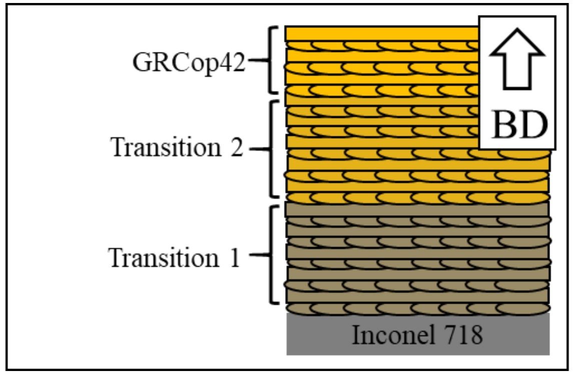

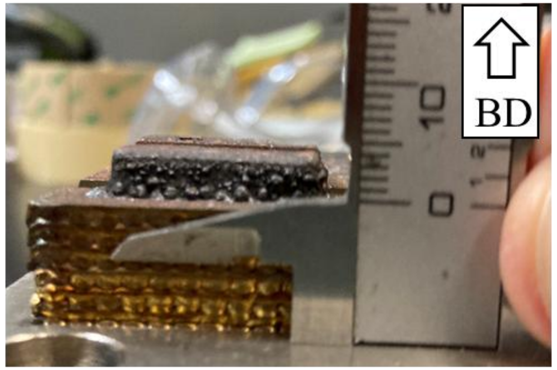

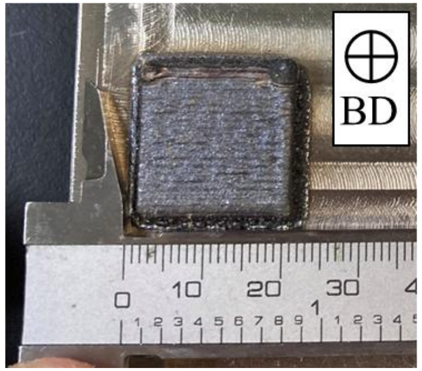

Material	Layer	Laser Power [W]
Inconel 718 wire	*All*	700
Transition 1	All	500
Transition 2	1-2	500
	3-5	600
	6	700
	7-8	800
	9	900
	10	1000
GRCop42	1-3	1050
	4-6	1100

Optical micrographs

- Optical microscopy of joint shows no evidence of islands / peninsulas: **No brittle phases**
- Trapped gas porosity found in the filler 1 composition: attributed to powder mixing.
- **NbO** found in the GRCop42: attributed to high O2 content.

Bimetallic joint

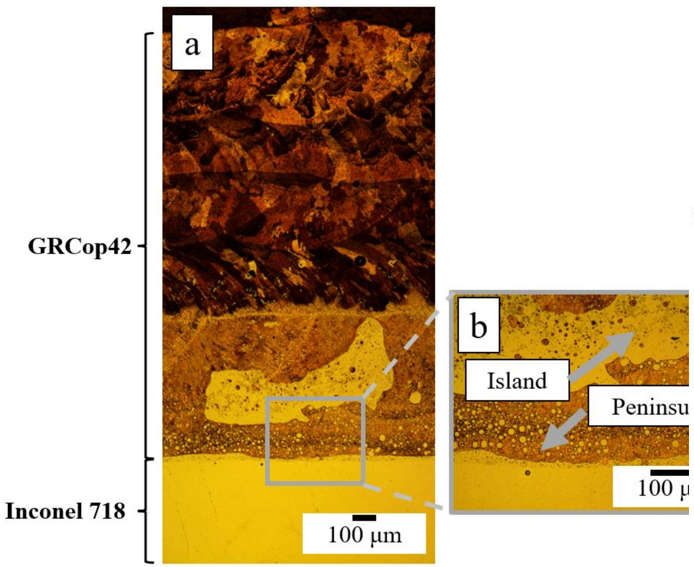

Joint with transition compositions

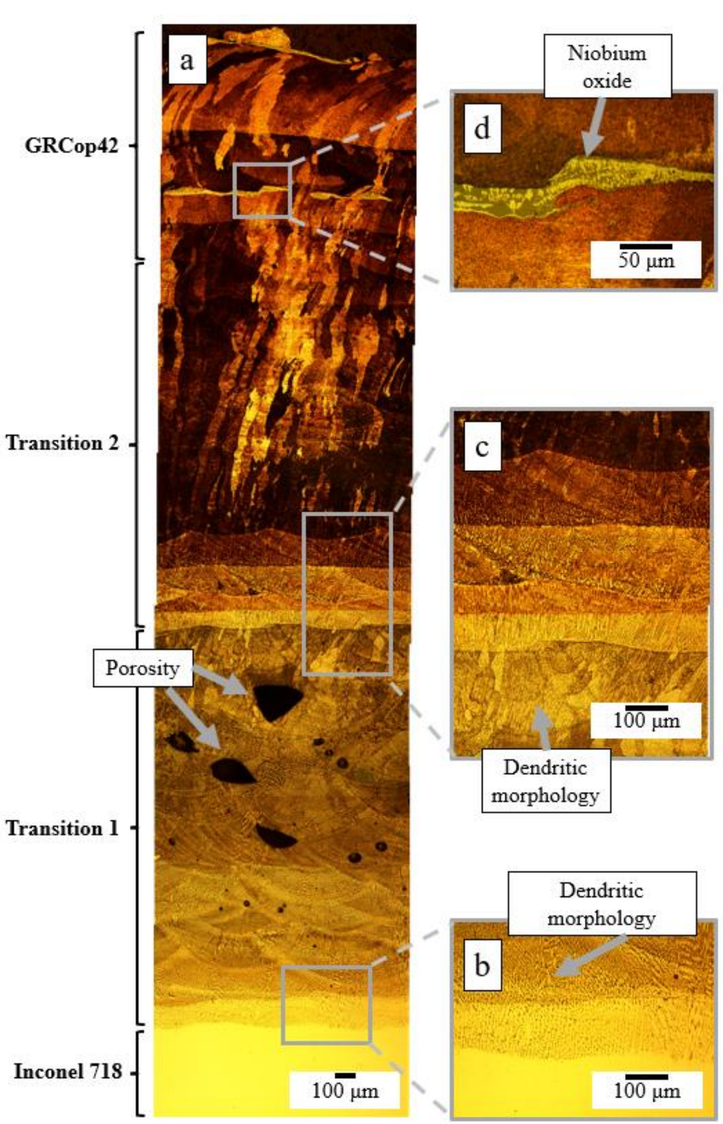

Microhardness

- Microhardness values of compositions in the LDED joint found to be higher than arc melted counterpart.
  - Attributed to higher cooling rate / decrease in grain size of the LDED joint.
- Gradient of microhardness observed at each compositional change.
  - Attributed to remelting and mixing between the deposited layer and substrate layer.
- Lowest microhardness observed in Filler 2.
  - 12.7% lower than for GRCop-42.

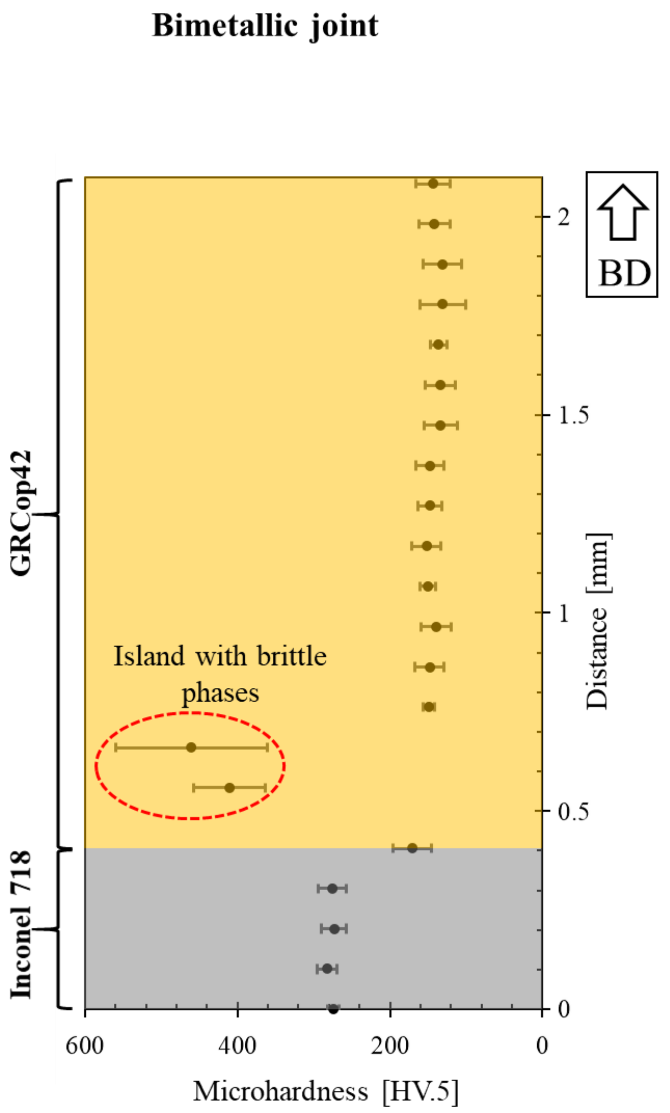

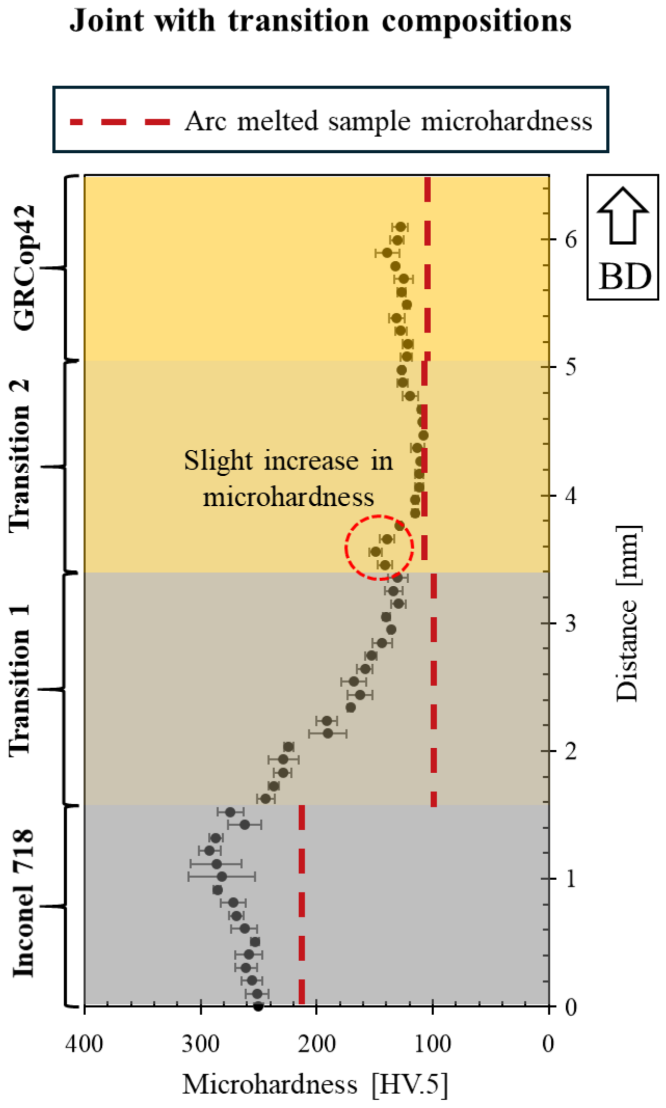

Conclusions

- Investigated the effect of travel speed on wire – LDED Inconel 625.
  - Higher travel speed increases yield when pulled parallel to BD; does not increase yield when pulled perpendicular to BD.
- Investigated metallurgy of Inconel 625 – GRCop42 mixtures
  - Liquid miscibility gap leads to a Cu-deprived liquid solidifying to form brittle crack inducing phases.
- Investigated bimetallic joining of Inconel 625 – GRCop42
  - Inconel 625 can be deposited onto GRCop42 without brittle phases, but depositing GRCop42 onto Inconel 625 results in brittle phase formation.
- Developed transition compositions to join Inconel 718 with GRCop42
  - Transition compositions avoid brittle phase formation.

Acknowledgements

- Advisor: Somayeh Pasebani
- Committee:
  - Dr. David McIntyre
  - Dr. Brian K. Paul
  - Dr. Julie Tucker
  - Dr. Donghua Xu
- Parents
- Dr. Peter Eschbach and Dr. Nick Wannenmacher
- Lab group and friends.

Questions?

Backup Slides

Calculating thermal gradient and solidification rate

$$R = \frac{VD}{L}$$

$$G = \frac{C_l}{R}$$

R – solidification rate
V – travel speed
D – depth of melt pool
L – length of melt pool

G – thermal gradient
C_l – cooling rate
R – solidification rate

SAD patterns of arc melted samples

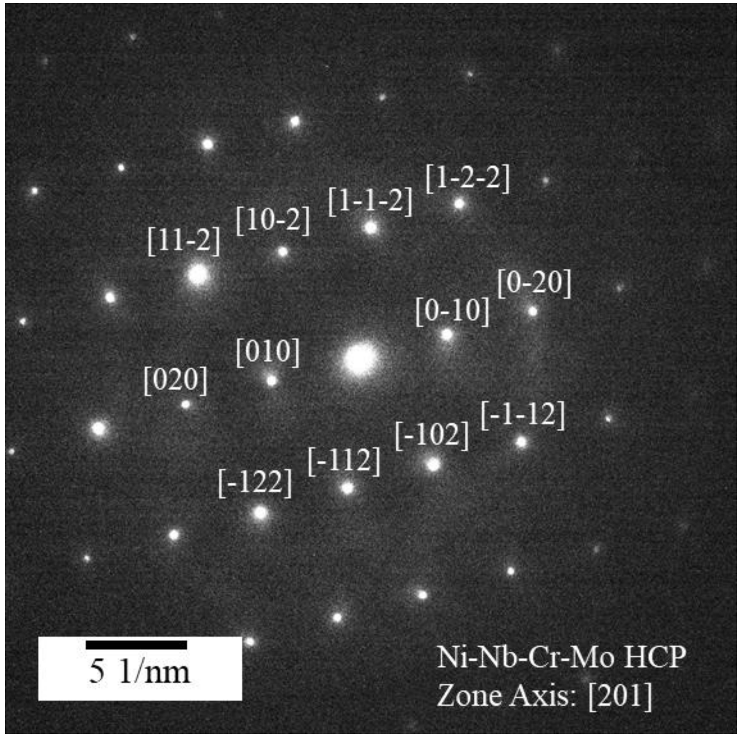

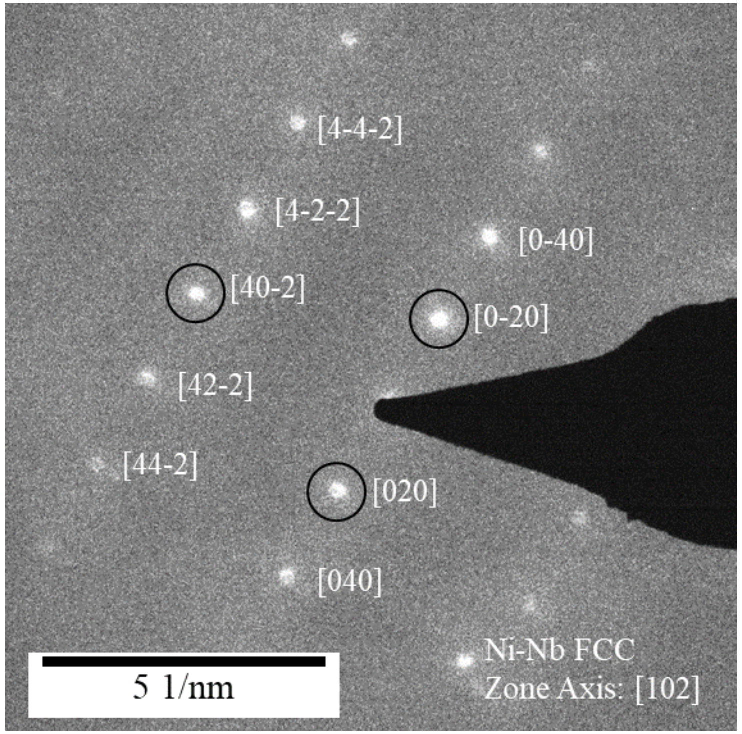

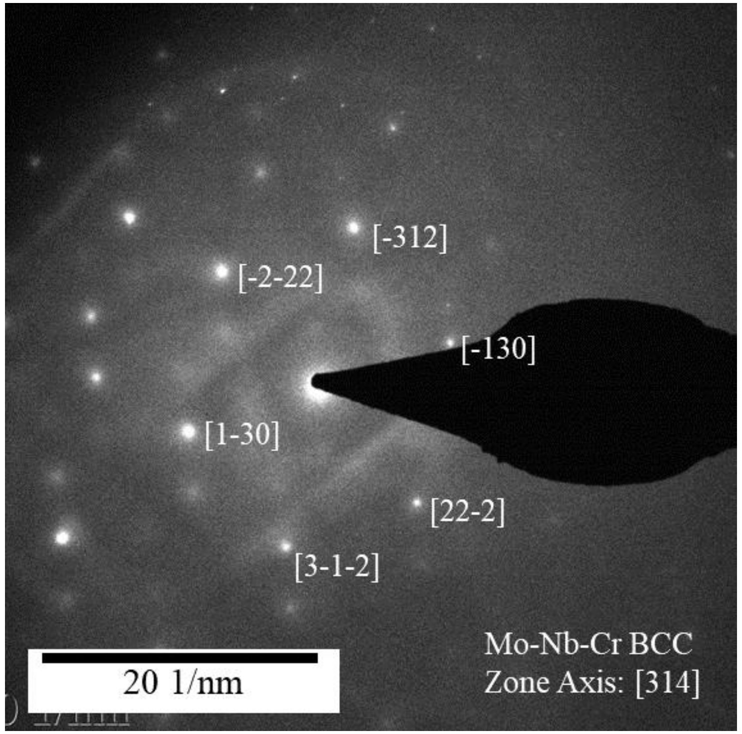

EBSD phase maps of arc melted samples

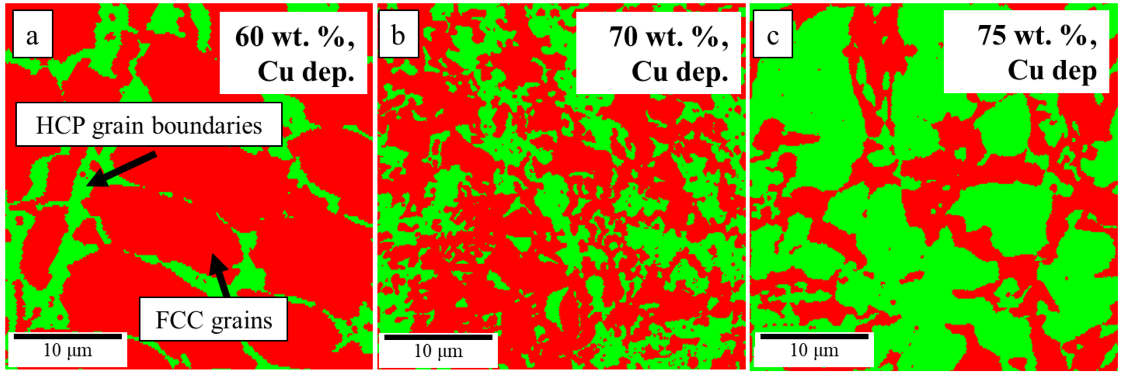

Ni-rich FCC	0.816 ± 0.102	0.584 ± 0.143	0.411 ± 0.090
HCP C14-Laves	0.184 ± 0.102	0.415 ± 0.143	0.588 ± 0.090
BCC α Mo-Nb-Cr	0	0	0
FCC $NiNb_5$	0	0	0

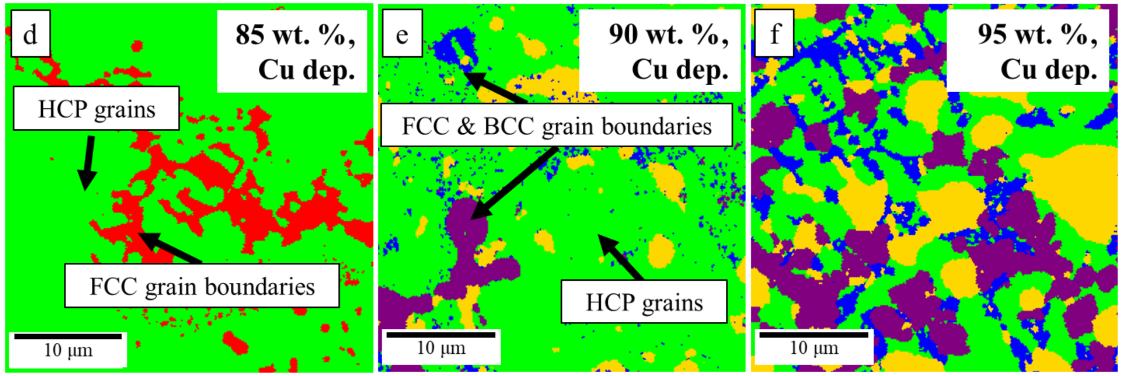

Ni-rich FCC	0.183 ± 0.259	0	0
HCP C14-Laves	0.816 ± 0.259	0.764 ± 0.323	0.486 ± 0.161
BCC α Mo-Nb-Cr	0	0.134 ± 0.194	0.363 ± 0.225
FCC $NiNb_5$	0	0.100 ± 0.189	0.150 ± 0.090

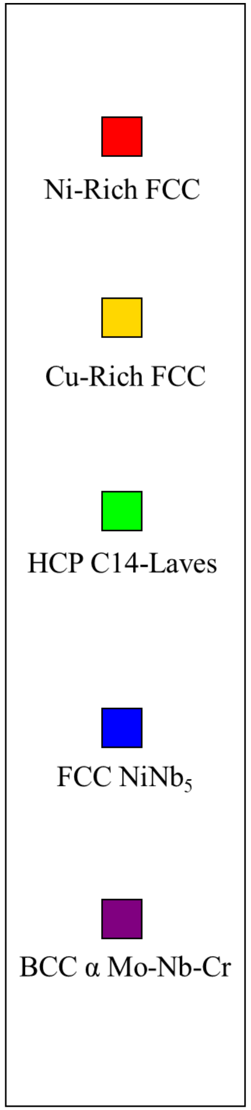

SAD patterns of LDED samples

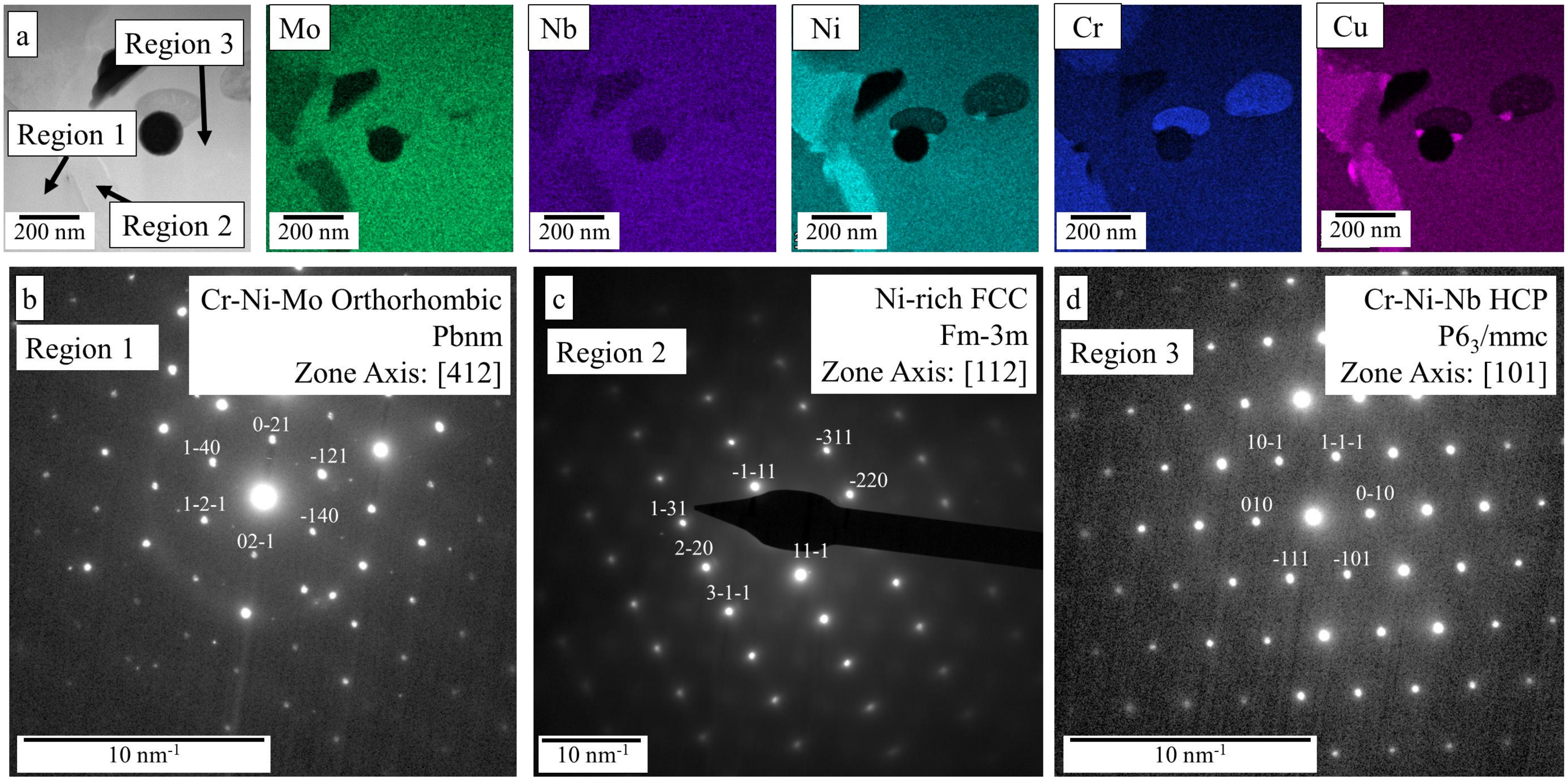

EBSD of bimetallic joint

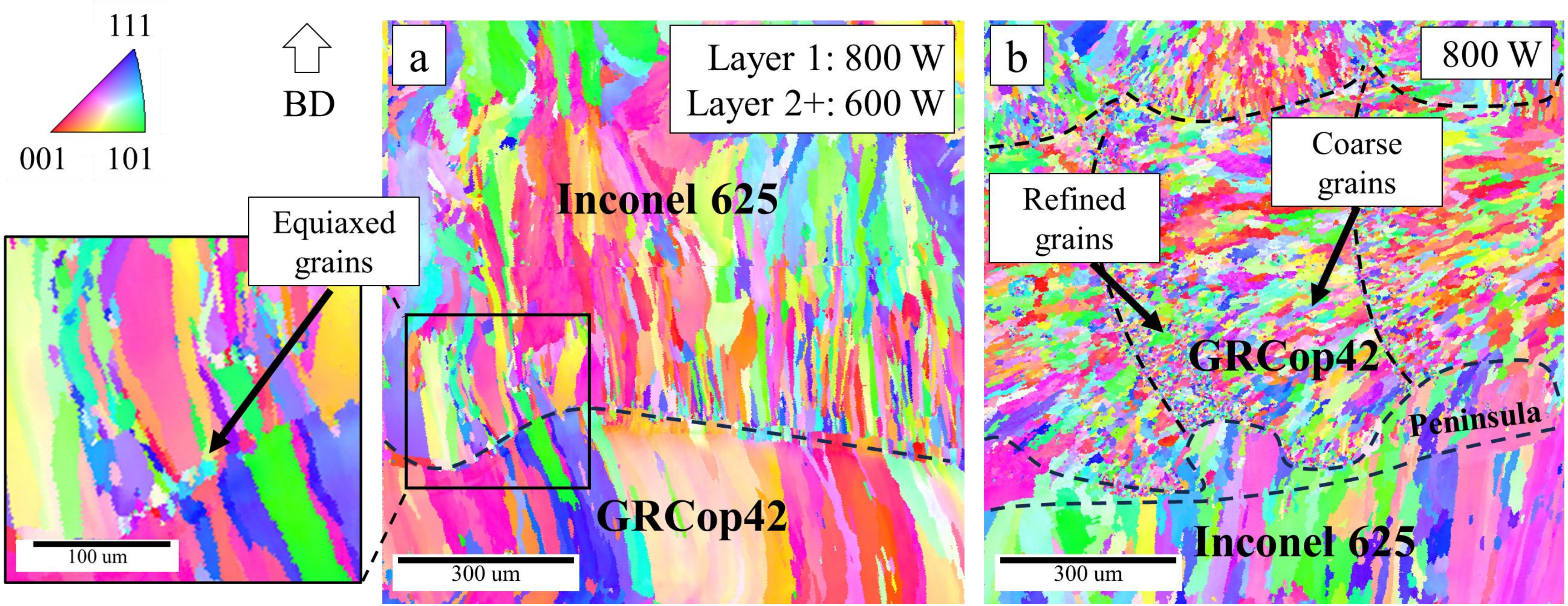

Backup: Solidification paths

Solidification path [A]:
60 wt. % Ni
20 wt.% GRCop42
20 wt.% Inconel 718

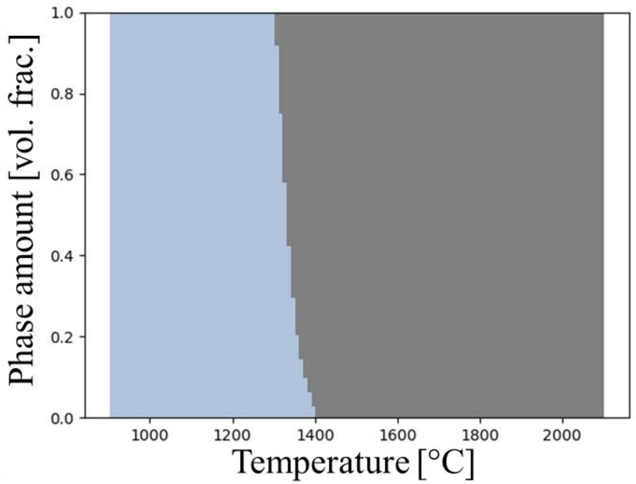

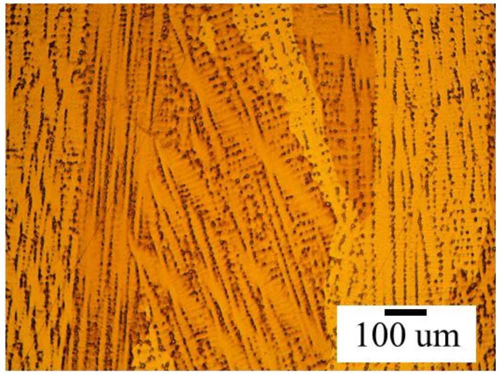

Solidification path [B]:
40 wt.% GRCop42
60 wt.% Inconel 718

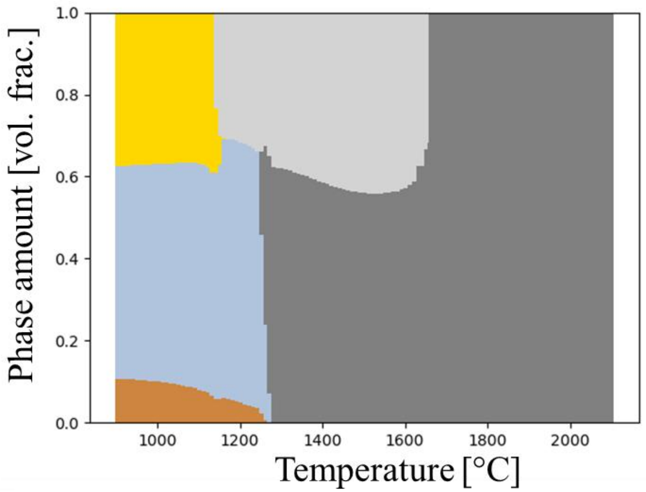

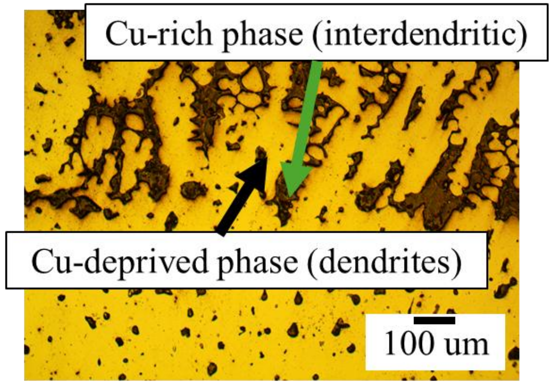

Solidification path [C]:
80 wt.% GRCop42
20 wt.% Inconel 718

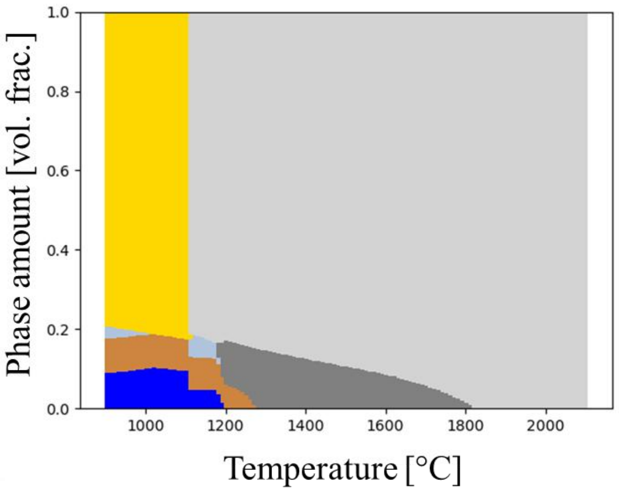

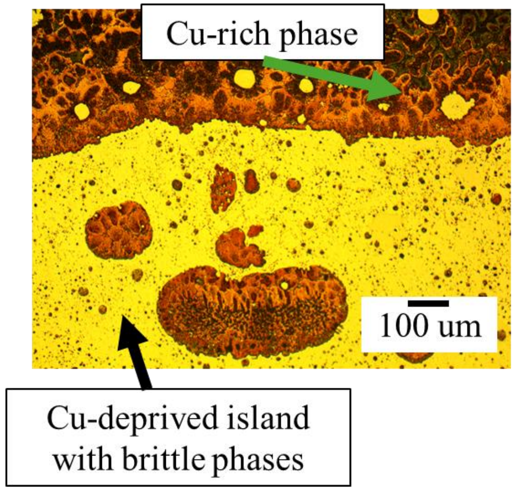

- Cu – rich FCC
- Cu – deprived FCC
- NbNi3 (δ)
- BCC_B2
- Cu – rich liquid
- Cu – deprived liquid

Compositional profile

- Deposited feedstock matches target composition towards the top of each compositional region.
  - This is a prerequisite to avoid the liquid miscibility gap.
- Gradient observed at each compositional change.
  - Attributed to remelting and mixing between the deposited layer and substrate layer.

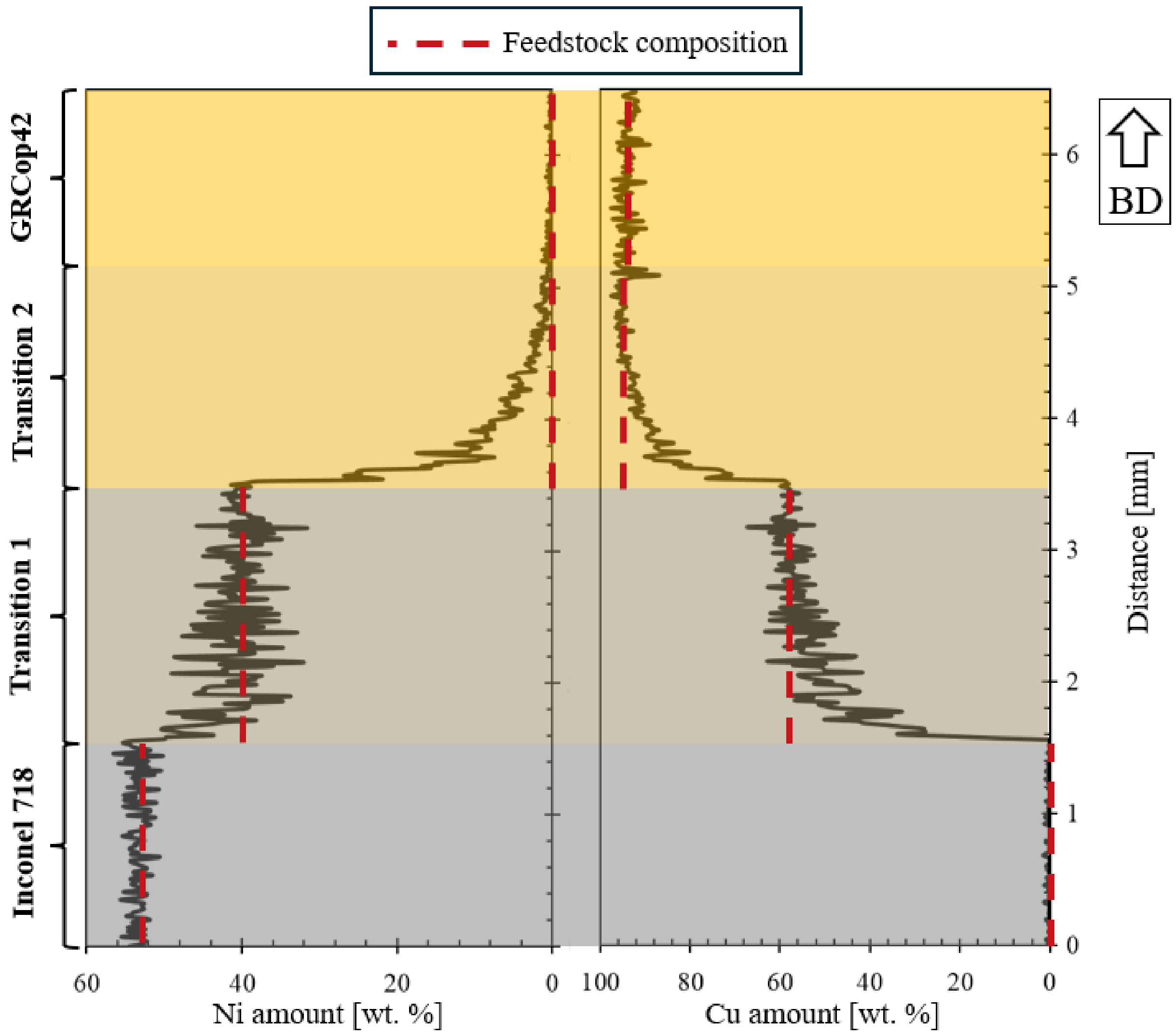

Grain morphology

- Epitaxial growth observed at every compositional change.
  - This stands in contrast to Inconel GRCop-42 bimetal samples, which show a lack of epitalixal growth.
- Columnar grains observed throughout most of the joint except above the filler 1 – filler 2 transition.
  - Attributed to an increased cooling rate in this layer.
- Large columnar grains observed in GRCop-42.
  - Attributed to high laser power utilized.

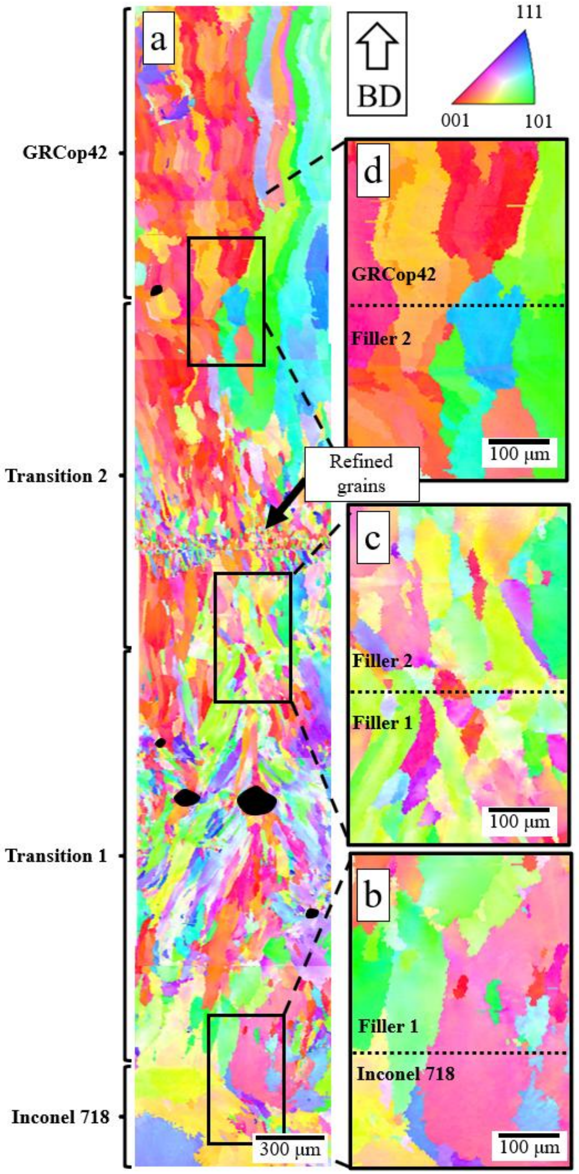

Oregon State University College of Engineering

Present phases

- Only FCC phases detected in the Inconel 718 Transition 1 regions.
- Expected C15 Cr_2Nb precipitates observed in the transition 2 GRCop42 regions.
- One peak corresponding to C14 Cr_2Nb observed.
  - This could be attributed to Ni migration at the interface.

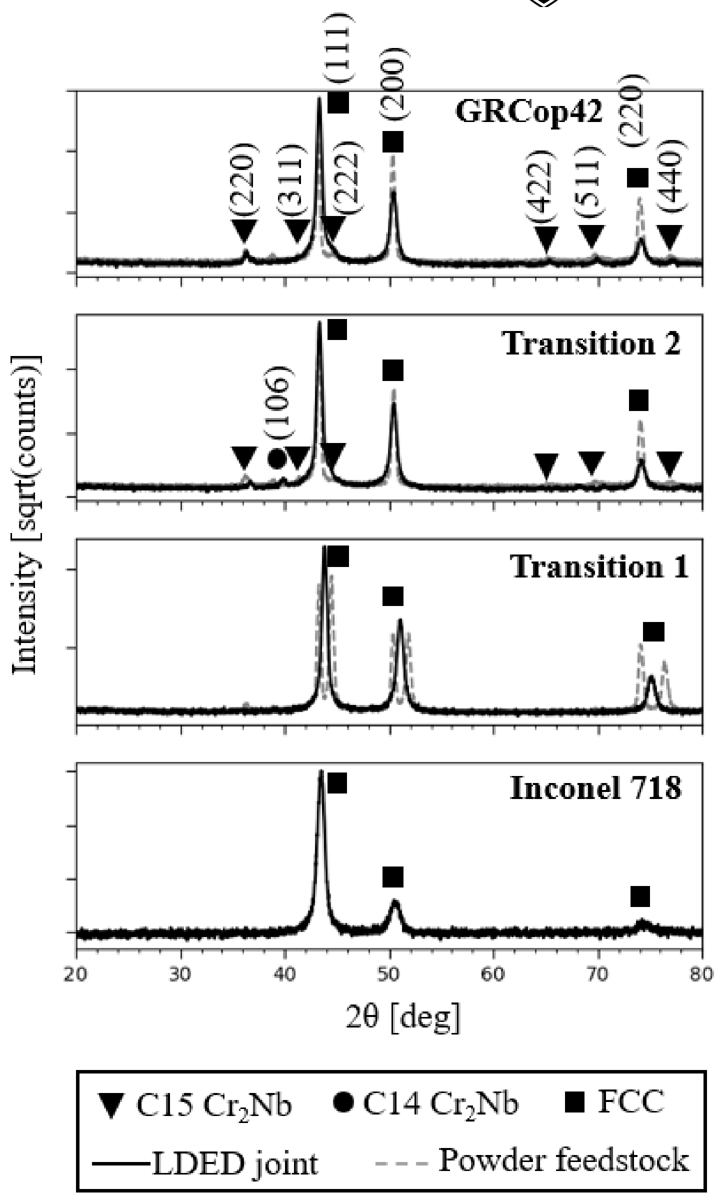

Inconel 625 onto GRCop42

- When depositing Inconel 625 onto GRCop42 at 600 W, lack of fusion observed in the first layer due to the GRCop42 acting as a heat sink.
- The lack of fusion is avoided by increasing the laser power in the first layer.
- Defect-free joint achieved – miscibility gap avoided by remelting less than 20 wt.% GRCop42.

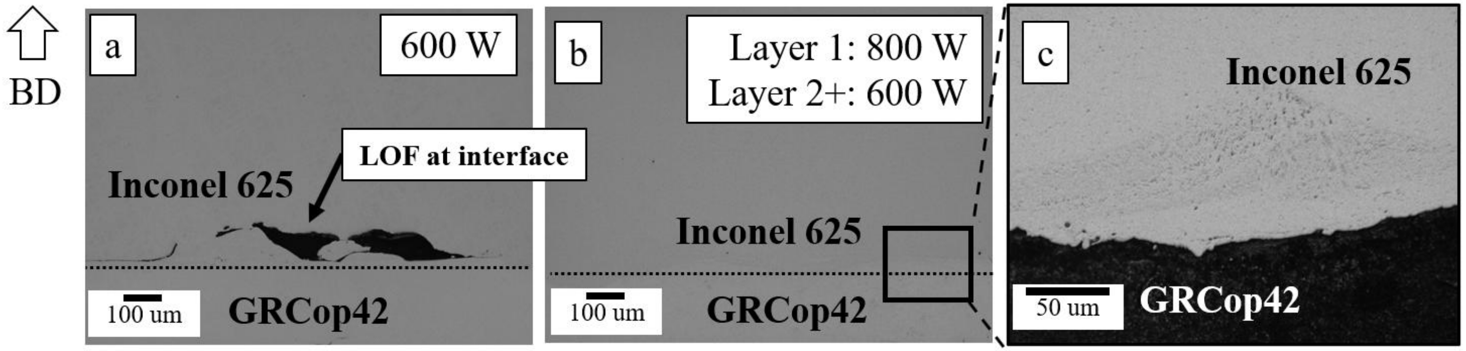

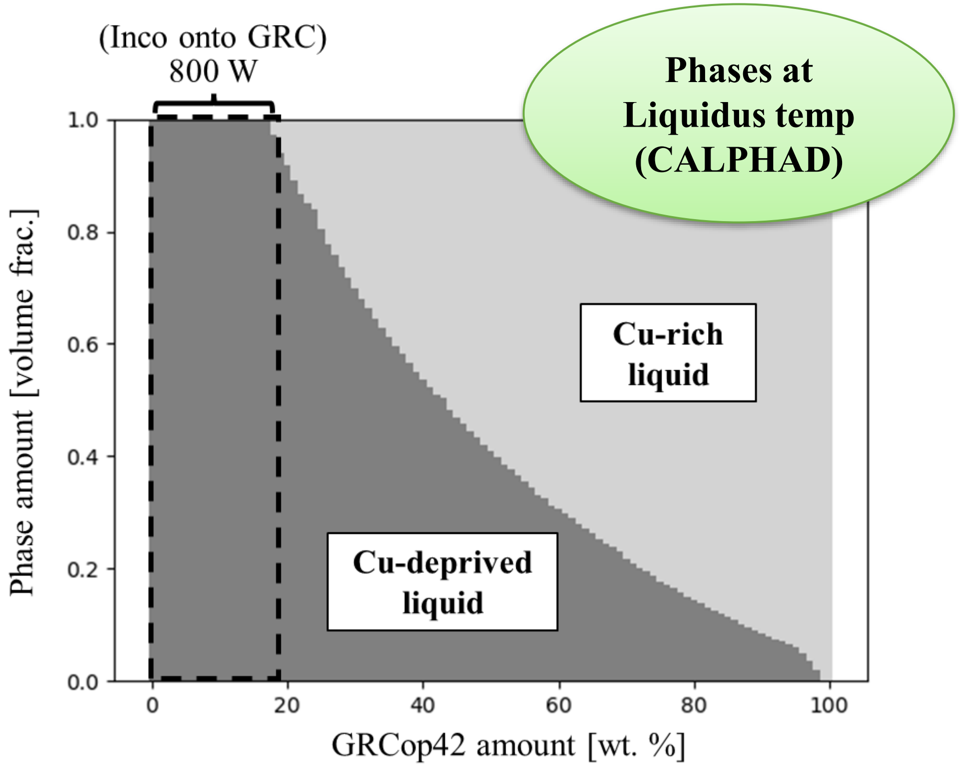

Preis et al., Effect of Liquid Miscibility Gap on Defects in Inconel 625–GRCop42 Joints through Analysis of Gradient Composition Microstructure (2024)